PORTLAND PRESS

BIOCHEMICAL JOURNAL
ACCEPTED MANUSCRIPT

Dynamic regulation of extracellular ATP in *Escherichia coli*

Alvarez, Cora Lilia, Corradi, Gerardo, Lauri, Natalia, Marginedas-Freixa, Irene, Leal Denis, María Florencia, Enrique, Nicolás, Mate, Sabina María, Milesi. Verónica. Ostuni. Mariano Anibal. Herlax. Vanesa. Schwarzbaum.

We studied the kinetics of extracellular ATP (ATPe) in *Escherichia coli*, and
their outer membrane vesicles (OMVs) stimulated with amphipatic peptides melittin (MEL) and mastoparan 7 (MST7). Real time luminometry was used to measure ATPe kinetics, ATP release and ATPase activity. The latter was also determined by following [^{32}P]Pi released from [γ-^{32}P]ATP. *E. coli* was studied alone, coincubated with Caco-2 cells or in rat jejunum segments. In *E. coli*, addition of [γ-^{32}P]ATP led to uptake and subsequent hydrolysis of ATPe. Exposure to peptides caused acute 3-fold (MST7) and 7-fold (MEL) increase of [ATPe]. In OMVs ATPase activity increased linearly with [ATPe] (0.1-1 μM). Exposure to MST7 and MEL enhanced ATP release by 3-7 fold, with similar kinetics to that of bacteria. In Caco-2 cells, addition of ATP to the apical domain led to a steep [ATPe] increase to a maximum, with subsequent ATPase activity. Addition of bacterial suspensions led to an 6-7 fold increase in [ATPe], followed by an acute decrease. In perfused jejunum segments, exposure to *E. coli* increased luminal ATP 2 fold. ATPe regulation of *E. coli* depends on the balance between ATPase activity and ATP release. This balance can be

Cite as Biochemical Journal (2017) DOI: 10.1042/BCJ20160879

Dynamic regulation of extracellular ATP in *Escherichia coli*

Authors:
Alvarez, Cora Lilia[1]
Corradi, Gerardo[1, 2]
Lauri, Natalia[1]
Marginedas-Freixa, Irene[8]
Leal Denis, María Florencia[1, 3]
Enrique, Nicolás[6, 7]
Mate, Sabina María[4, 5]
Milesi, Verónica[6, 7]
Ostuni, Mariano Anibal[8]
Herlax, Vanesa[4, 5]
*Schwarzbaum, Pablo Julio[1, 2]

Affiliations:
1 Instituto de Química y Fisico-Química Biológicas "Prof. Alejandro C. Paladini", UBA, CONICET, Facultad de Farmacia y Bioquímica. Junín 956. Buenos Aires, Argentina.

2 Universidad de Buenos Aires. Facultad de Farmacia y Bioquímica. Departamento de Química Biológica. Cátedra de Química Biológica Superior. Buenos Aires, Argentina.

3 Universidad de Buenos Aires. Facultad de Farmacia y Bioquímica. Departamento de Química Analítica y Fisicoquímica. Cátedra de Química Analítica. Buenos Aires, Argentina.

4 Instituto de Investigaciones Bioquímicas de La Plata "Prof. Dr. Rodolfo R. Brenner" UNLP, CONICET, Facultad de Ciencias Médicas. Calle 60 y 120. La Plata, Argentina.

5 Universidad Nacional de La Plata. Facultad de Ciencias Médicas. La Plata, Argentina.

6 Instituto de Estudios Inmunológicos y Fisiopatológicos UNLP, CONICET, Facultad de Ciencias Exactas. Calle 115 y 47. La Plata, Argentina. .

7 Universidad Nacional de la Plata. Facultad de Ciencias Exactas. Departamento de Ciencias Biológicas. Cátedra de Fisiología. La Plata, Argentina.

8 UMR-S1134, Integrated Biology of Red Blood Cells, Inserm, Université Paris Diderot, Sorbonne Paris Cité, Institut National de la Transfusion Sanguine, Laboratoire d'Excellence GR-Ex, F-75015 Paris, France.

*corresponding author. Email: pjs@qb.ffyb.uba.ar
Correspondence:
IQUIFIB – INSTITUTO DE QUÍMICA Y FISICOQUÍMICA BIOLÓGICAS
Facultad de Farmacia y Bioquímica, Universidad de Buenos Aires Junin 956 – C1113AAD. BUENOS AIRES, ARGENTINA
Tel.Nr.5411 4 964 8289
Fax Nr.5411 4 9625457

ABSTRACT

We studied the kinetics of extracellular ATP (ATPe) in *Escherichia coli*, and their outer membrane vesicles (OMVs) stimulated with amphipatic peptides melittin (MEL) and mastoparan 7 (MST7).

Real time luminometry was used to measure ATPe kinetics, ATP release and ATPase activity. The latter was also determined by following [^{32}P]Pi released from [γ-^{32}P]ATP. *E. coli* was studied alone, coincubated with Caco-2 cells or in rat jejunum segments. In *E. coli*, addition of [γ-^{32}P]ATP led to uptake and subsequent hydrolysis of ATPe. Exposure to peptides caused acute 3-fold (MST7) and 7-fold (MEL) increase of [ATPe]. In OMVs ATPase activity increased linearly with [ATPe] (0.1-1 μM). Exposure to MST7 and MEL enhanced ATP release by 3-7 fold, with similar kinetics to that of bacteria. In Caco-2 cells, addition of ATP to the apical domain led to a steep [ATPe] increase to a maximum, with subsequent ATPase activity. Addition of bacterial suspensions led to an 6-7 fold increase in [ATPe], followed by an acute decrease. In perfused jejunum segments, exposure to *E. coli* increased luminal ATP 2 fold.

ATPe regulation of *E. coli* depends on the balance between ATPase activity and ATP release. This balance can be altered by OMVs, which display their own capacity to regulate ATPe. *E. coli* can activate ATP release of Caco-2 cells and intestinal segments, a response which in vivo might lead to intestinal release of ATP from the gut lumen.

SUMMARY STATEMENT

We explored the processes governing the time-dependent accumulation of extracellular ATP of *Escherichia coli* stimulated by the amphipatic peptides mastoparan 7 and melittin. We analyzed extracellular ATP regulation of *E. coli*, and their outer membrane vesicles.

SHORT TITLE

Regulation of extracellular ATP in *Escherichia coli*

KEYWORDS

EXTRACELLULAR ATP REGULATION
Escherichia coli
MASTOPARAN 7
MELITTIN
OUTER MEMBRANE VESICLES
Caco-2 CELLS

INTRODUCTION

In bacteria, as in most cell types and organisms, cytosolic adenosine triphosphate (ATPcyt) acts as an “energy currency”; a regulated variable providing energy for metabolic reactions, serving as substrate for nucleic acid synthesis, and regulating a variety of biological processes.

In *Escherichia coli* ATPcyt concentration ranges from 1 to 5 mM, depending on the environmental and physiological conditions [1-3]. The nucleotide is synthesized *de novo* or obtained from external purine compounds by salvage pathways [4].

ATPcyt of *E. coli* can be transported through the inner membrane (IM) to the periplasm, where it can be metabolized by various enzymes [5]. The resulting adenosine and adenine can be transported back through exchangers to the cytoplasm [4]. Alternatively, periplasmic ATP, as well as ADP, AMP and other small hydrophilic solutes, can diffuse across the outer membrane (OM) through water filled porins which are permeable to solutes smaller than 600-700 Da [6-7]. At neutral pH ATP is mainly an anionic species of 507 Da capable of crossing the OM via one or more porins whose selectivity on the basis of chemical structure is poor [7-9].

Thus, there may be a dynamic exchange allowing ATP to be released from the periplasm or be taken up from the extracellular space. In agreement with these findings, extracellular ATP (ATPe) accumulated in nano- to low micromolar concentrations in *E. coli* cultures under different experimental conditions [10-12].

E. coli possesses periplasmic nucleotidases and phosphatases capable of hydrolyzing ATP [5,13]. An enzyme encoded by the *ushA* gene displayed 5’-nucleotidase activity in *E. coli* [5,14], facilitating the hydrolysis of ATP, ADP, AMP and other 5’ribo and 5’deoxyribonucleotides [15]. In addition, there are at least two periplasmic phosphatases capable of dephosphorylating ATP: AphA, an acid phosphatase exhibiting hydrolytic activity in an acid milieu [16] and PhoA, an alkaline phosphatase, exhibiting activity at pH 7-9. PhoA can be either transcriptionally upregulated in the absence of Pi [17] or kinetically inhibited by high Pi [18,19].

Bacterial release of ATP may occur by lytic and non lytic mechanisms. In *E. coli*, hypotonic treatment, carbon starvation as well as exposure to glucose or carbon monoxide promote the non lytic release of ATP and other solutes [12,20,21]. Repression of 5'nucleotidases, on the other hand, leads to basal excretion of purine nucleotides, although ATP export was not tested [5].

Amphipatic peptides can enhance the permeability to small solutes in a variety of cells [9,22-30], either by creating disordered regions of the lipid bilayer and/or by forming pores [31-35]. Among these are small amphipatic peptides belonging to the families of mastoparans and melittins, which display a broad spectrum of lytic activities in a variety of cells [36,37], inducing ATP release in erythrocytes [38,39] and adrenal chromaffin cells [40]. Mastoparans exhibit antimicrobial activity against both Gram-positive and -negative bacteria tested, though in *E. coli* the OM had to be previously disrupted in order for mastoparan to be effective [22,23].

Melittin, on the other hand, was rapidly taken up by *E. coli*, inducing morphological changes usually followed by leakage of the cytoplasm [9,37].

In principle, [ATPe] of *E. coli* may increase by cytoplasmic/periplasmic ATP release induced by physiological and pharmacological stimuli, and/or decrease by ATPe hydrolysis due to periplasmic nucleotidases.

Thus in this study we evaluated the relative contribution of ATPe hydrolysis and ATP release to the dynamic regulation of ATPe of *E. coli*. Melittin and Mastoparan 7 (an active mastoparan analogue; [41]) were used as ATP release inducers.

E. coli are able to form and release outer membrane vesicles (OMVs) both *in vivo* and *in vitro* [42-44]. Since the lumen of these vesicles may contain ATP as well as nucleotidases of periplasmic origin [45,46], our analysis of the dynamic ATPe regulation of *E. coli* took the contribution of OMVs into account.

Finally, we analyzed ATPe regulation in a condition closer to the *in vivo* situation, where *E. coli* lives as a commensal of the gut lumen, in close contact with intestinal epithelial cells. Accordingly, we studied the effect of *E. coli* on ATPe regulation of the human intestinal Caco-2 cell line and rat intestinal segments.

MATERIALS AND METHODS

1. Chemicals

All reagents were of analytical grade. Mastoparan 7 (MST7), Mastoparan 17 (MST17), Melittin (MEL) and firefly luciferase (EC1.13.12.7) were purchased from Sigma-Aldrich (St. Louis, MO, USA). D-luciferin was obtained from Molecular Probes Inc. (Eugene, OR, USA). [γ ^{32}P]ATP (10 Ci/mmol) was purchased from Perkin Elmer Life Sciences (Santa Clara, California, USA). Phosphatidylglicerol, cardiolipin and phosphatidylethenolamine were purchased from Avanti Polar Lipids (AL, USA).

2. Bacterial strains and culture conditions

Escherichia coli DH5α were used in all experiments using bacteria and OMVs, the only exception being the experiments run to assess β-galactosidase activity (see section 12 M&M), where *E. coli* BL21 (DE3) were used. Both strains showed similar responses to MST7 and MEL (Supplementary Figure 1).

E. coli were cultured overnight in Luria–Bertani (LB) broth at 37°C, with shaking at 220 rpm. Overnight cultures were diluted 1:100 in fresh LB broth and cultured at 37 °C with shaking. Growth was monitored by optical density at 600 nm (OD_{600}). Bacteria were harvested when an OD_{600} of 0.6-0.9 was attained. Bacterial cultures were then centrifuged 2,500 g for 5 min, the supernatant was removed and the pellet resuspended at $2x10^9$ bacteria/ml in M9 medium containing: Na_2HPO_4 42.3mM; KH_2PO_4 22.1 mM; NH_4Cl 18.7 mM; $MgSO_4$ 7 μM; NaCl 108 mM and $CaCl_2$ 0.1 mM; pH 7. Centrifugation and washing of the pellet was repeated 3 times.

For experiments run in the absence of phosphate, overnight cultured bacteria were harvested, washed and resuspended in a similar way, except that Hepes medium (10 mM; ClK 1 mM; NaCl 140 mM; pH = 7) was used.

In most cases, bacterial suspensions were preincubated in M9 or Hepes media for 60 min before use. In a few experiments (see section 6 below), intact jejunum segments were exposed to supernatants collected from *E. coli* suspensions. In this case, *E. coli* were cultured in LB medium as above, centrifuged, and the resulting supernatant was collected.

3. Isolation of outer membrane vesicles (OMVs)

Bacteria were cultured as above and OMVs were isolated from bacterial culture supernatants as described before [47]. Bacteria were then pelleted (2,500 g for 10 min at 4ºC), and culture supernatants filtered using 0.22 µm pore size filters (Millipore Corporation, Billerica, MA, USA), followed by centrifugation at 100,000 g for 2 h at 4ºC. The resulting pellet containing the OMVs was diluted in M9 medium, and held at 4ºC for up to 48 h before use. An aliquot was withdrawn to determine protein content by the Bradford assay. Total lipids of OMVs were extracted using a standard procedure [48] and subjected to analysis by high-performance TLC, using the following solvent system: chloroform/ methanol/2,propanol/0.25% KCl-ethylacetate (30+9+25+6+18). Lipid spots were detected by spraying with sulfuric acid/ethanol (5:100, v/v) and charring at 120˚C. Phosphatidylglicerol (PG), cardiolipin (CL), phosphatidylethenolamine (PE) and lypopolisacharide were used as standards. Preliminary experiments showed that ATPase activity (assayed by the two methods described below, section 10 M&M) of OMVs were similar for suspensions stored for 24 or 48 h at 4ºC before use (data not shown).

Aliquots of OMVs suspensions (10 µl) were spotted on LB agar plates for overnight culture at 37°C. No bacterial colonies were found.

4. Electron microscopy.

OMVs were observed by electron microscopy. Vesicles were fixed with 1% (v/v) glutaraldehyde for 45 min at room temperature, centrifuged (100,000 g for 2.5 h at 4ºC) and resuspended in 0.1M ammonium acetate buffer (pH=7). A drop of fixed vesicles was applied to a 400-mesh copper grid covered with a carbon film and the samples were stained with 2% (w/v) phosphotungstic acid (pH 5.2 with KOH). Electron micrographs were taken at 50,000 X magnification.

5. Culture of Caco-2 cells.

Caco-2 cells (passages 5–10, ATCC, Molsheim, France) were seeded on Snapwell tissue culture-treated polycarbonate membrane filters (6.5 mm diameter and 0.4 µm pore size; Corning, New York, USA). Cells were grown for 15-30 days on Dulbecco's modified Eagle's medium containing 4.5 g/L glucose

supplemented with 10% v/v fetal bovine serum, 2 mM L-glutamine, and antibiotics in a humidified atmosphere of 5% CO_2 at 37°C. Experiments were performed on confluent cells that had developed a transepithelial electrical resistance greater than 250 w/cm^2. Under this condition, cells formed a polarized epithelial cell monolayer with distinguished apical and basolateral domains. Membrane permeability was tested by adding dextran-FITC (MW = 59,000-77,000 Da, Sigma,) to the upper chamber (apical side) and measuring fluorescence (exc/emi 490/520 nm) on the lower chamber (basolateral side).

6- Rat intestinal perfusates.

Adult Wistar rats of either sex of 250–350 g body weight were anesthetized. Jejunum segments (approx. 10 cm long) were excised from animals and immediately placed in cold Ringer buffer containing (in mM): NaCl 130, KCl 4.7, KH_2PO4 1.2, $CaCl_2$ 2.5, $MgSO_4$ 1.2, $NaHCO_3$ 24, glucose 6, oxygenated with a mixture of 95% O_2 and 5% CO2, pH 7.4. The intestinal segment was flushed of luminal contents and placed in an organ bath containing 10 ml of Ringer solution kept at room temperature. The proximal and distal ends of the jejunum were cannulated to allow slow infusion of Ringer solution at 37 ºC with a flow rate of 1 ml/min using a peristaltic pump (Model E50, Elmeco Laboratory Instruments).

During the first 30 min the tissue was infused with Ringer solution and then replaced by a bacterial suspension, containing 5x10^8 bacteria/ml in the same saline solution. Samples were collected at the distal end every 10 min during 60 min and the luminal ATP (ATP_L) was measured by off-line luminometry immediately after sample collection. In some experiments, before replacing Ringer solution by the bacterial suspension, supernatants collected from *E. coli* suspensions were perfused.

7. Treatments

ATPe kinetics of *E. coli* was assessed when bacteria were exposed to Mastoparan 7 (MST7) or melittin (MEL). α,β-Methyleneadenosine 5′-triphosphate lithium salt (AMP-CPP, a non hydrolyzable ATP analogue) was used as inhibitor of ATPase activity by one or more enzymes.

ATPe kinetics of Caco-2 cells under exposure to bacteria (*E. coli*) or to an adrenergic cocktail denoted as 3V, which contained 10 µM isoproterenol (a β-adrenergic agonist), 30 µM forskolin (an adenylate kinase activator) and 100 µM papaverine (a phosphodiesterase inhibitor). 3V was used to induce a fast increase of cytosolic cAMP. Experiments with Caco-2 cells exposed to either bacteria or 3V were carried out in the absence or presence of carbenoxolone, an inhibitor of ATP release.

Intact jejunum segments were continuously infused with either *E. coli* suspensions or supernatants collected from *E. coli* suspensions, and the perfusates were used for ATP determination by off-line luminometry.

8. Extracellular ATP

ATPe was measured by real-time luminometry with bacteria, OMVs and Caco-2 cells using firefly luciferase, which catalyzes the oxidation of luciferin in the presence of ATP to produce light. In experiments using rat intestinal segments, the presence of ATP in the intestinal lumen was assessed by off-line luminometry. A custom-built luminometer of high sensitivity was used [49-50].

8.1 Online luminometry

8.1.1 *E. coli* and OMVs

Real-time luminometry was carried out with bacteria or OMVs laid on coverslips that were mounted in the assay chamber of the luminometer. Measurements were performed in M9 medium containing a luciferin-luciferase mixture at 20°C. $2x10^7$ bacteria/40µl or 10 µl OMVs (0.8-1.4 µg protein)/100 µl were used.

The time course of light emission was transformed into ATPe concentration versus time by means of a calibration curve. Increasing concentrations of ATP from 4 to 974 nM were sequentially added to the assay medium from a stock solution of ATP dissolved in M9 medium. In results of Figure 4C, the instantaneous rate of [ATPe] change (denoted as P_{ATP}) was calculated by taking the first derivative of the experimentally observed ATPe kinetics of Figures 4A and B.

8.1.2 Caco-2 cells

Caco-2 cells were grown and polarized on permeable supports as described in section 5 above. Real-time luminometry was carried out by placing these supports –containing approx. $5x10^5$ cells- in the assay chamber of the luminometer. The configuration of the setup is illustrated in Supplementary Figure 2. Measurements were run at 20°C. The basolateral side was loaded with 40 µl of DPBS medium (Gibco™), while the apical side was loaded with 40 µl of DPBS medium containing a luciferin-luciferase mixture. Using this configuration the light emitting luciferase reaction occurs in the apical domain.
The time course of light emission was transformed into ATPe concentration versus time by means of a calibration curve. Increasing concentrations of ATP (24-875 nM) were sequentially added to the assay medium from a stock solution of ATP dissolved in DPBS medium. Results were expressed as [ATPe] at every time point of a kinetic curve.
Increases in [ATPe] were evaluated as the difference between [ATPe] at 1 min post stimulus and the basal [ATPe], and are indicated as ΔATP_1.

8.2 Off-line luminometry of rat intestinal perfusates

Aliquots (45 µL) of perfusates, were taken every 10 minutes, containing 0 (control) or $5x10^8$ bacteria /mL and used to measure ATP_L. A standard ATP curve was obtained for each sample by adding 1 µL of increasing concentrations of ATP from 1 to 20 µM. For each experiment, concentrations of ATP_L were normalized to the controls conditions in the absence of bacteria.

9. Intracellular ATP

The intracellular ATP content of *E. coli* was estimated in real-time measurements. Briefly, 10 µl of a bacterial suspension ($2x10^8$ bacteria) were placed on coverslips. Samples were desiccated at room temperature to induce bacteriolysis [32]. The desiccated residue was dissolved in 40 µl, and the total content of ATP was measured by luminometry as described for ATPe (section 8.1).

10. Hydrolysis of ATPe

The rate of ATPe hydrolysis was tested in bacteria, OMVs and polarized Caco-2 cells. It was determined by following the accumulation of [^{32}P]Pi release from exogenous [γ-^{32}P]ATP, and by real-time luminometry.

10.1 [γ-^{32}P]ATP technique [38,51]

It was used for bacteria, OMVs and Caco-2 cells. The reaction was started by adding [γ-^{32}P]ATP (0.27 Ci/mmol; from 100 to 1,000 nM) to bacterial- or OMVs suspensions at 20°C. At different times, 100 µL aliquots of the suspension were withdrawn by duplicate and were poured into 750 µL of a stop solution containing 4.05 mM $(NH_4)_6Mo_7O_{24}$ and 0.83 mM $HClO_4$ (molybdate-perchloric solution). The ammonium molybdate solution formed a complex with the released phosphate, which was then extracted with 0.6 mL of isobutyl alcohol. Phases were separated by centrifugation at 1,000 ×g for 5 min, aliquots of 200 µL of the organic phase containing [^{32}P]Pi were transferred to vials with 2 mL of 0.5 M NaOH and radioactivity was measured by the Cerenkov effect. Any hydrolysis of [γ-^{32}P]ATP into ADP + [^{32}P]Pi in the bacterial- or OMVs suspensions can be defined as ATPase activity; the time course of [^{32}P]Pi accumulation yields a measure of the rate at which one or more nucleotidases or phosphatases of the samples hydrolyze ATPe.

To calculate ATPase activity, time dependent levels of Pi were fitted to

$$Y = Y0 + A\cdot(1-\exp^{-k.t}) \qquad \text{(Eq. 1)}$$

where Y and Y0 are the values of [^{32}Pi] at each time (t) and at t = 0, respectively; A represents the maximal value for the increase in Y with time and k is a rate coefficient. The parameters of best fit resulting from the regression were used to calculate the initial rate of ATPase activity (vi) as k × A (i.e. the first derivative of Eq. (1) evaluated at t = 0). The [^{32}Pi] Pi moles produced from [γ-^{32}P]ATP were calculated using the ATP specific activity.

In a few experiments, instead of using submicromolar ATP concentrations, ATPase activity was detected at 500 µM ATP to provide an estimate of apparent maximal ATPase activity (Vi).

ATPase activity was expressed as: pmol/(10^{10} bacteria min) in *E. coli* suspensions, pmol/(µg prot) in OMVs or nM/min in Caco-2 cells.

10.2 Uptake and hydrolysis of ATPe in *E. coli*

E. coli has cytosolic and periplasmic compartments. Unless otherwise stated, by uptake of ATPe we mean that ATPe should enter the periplasm, irrespective of its final location or metabolism inside the bacterium.

Aliquots (100 µl) of *E. coli* suspensions were incubated with 1 µM [γ-^{32}P]ATP for 2 or 30 min, after which they were diluted in 1.4 ml of cold M9 medium, and centrifuged 5 min at 2400 g. The resulting pellets were treated in two different ways: 1- they were transferred to vials containing 2ml of 0.5 M NaOH. This provided a measure of total radioactivity being taken up by bacteria, irrespective of ATP hydrolysis, 2- pellets were first resuspended in M9 medium, centrifuged 1 min at 2400 g and the resulting pellet dissolved in 600 µL of a molybdate-percholoric solution, and treated as described for ATPase activity measurements. That is, the solution was extracted with 0.48 mL of isobutyl alcohol and molybdate-percholoric phases were separated by centrifugation. Aliquots of both phases were transferred to vials with 2 ml of 0.5 M NaOH. The organic phase was used to determine the amount of [^{32}Pi]Pi produced from [γ-^{32}P]ATP, while the molybdate-perchloric phase was used to determine the amount of [γ-^{32}P]ATP remaining after hydrolysis. Radioactivity was measured by the Cerenkov effect.

10.3 ATPe hydrolysis by real-time luminometry

This method was used for studies with OMVs and Caco-2 cells.

OMVs. Coverslips with 10 µl of OMVs suspensions were mounted in the measuring chamber of the luminometer and exposed to luciferase reaction mixture. Light emission was measured for 10 min, ATP was then added to the chamber at final concentrations of 200, 600 and 1,000 nM (in separate experiments) and measurements were carried out for another 30 min.

Light output was transformed into ATPe concentration vs. time by means of a calibration curve and the slope of disappearance of ATPe (vi) was estimated from ATPe kinetics and multiplied by -1. ATPase activity was expressed as nM/(µg prot min).

Caco2 cells. Measurements were done on the apical side of polarized cells held on permeable supports as described in section 5.

Basal light emission was measured for 5 min, ATP (0.2-7μM) or aliquots of *E. coli* suspensions were then added to the upper chamber at a given concentration and measurements were carried out for another 15-20 min. Light output was transformed into ATPe concentration vs. time by means of a calibration curve (section 8.2) and the slope of disappearance of ATPe (vi) was estimated from the maximum value of the ATPe kinetics until the end of the experiment, and multiplied by -1. ATPase activity was expressed as nM/min.

11. Hydrolysis of p-Nitrophenyl Phosphate.

p-Nitrophenyl Phosphate (pNPP) was used as a substrate to estimate periplasmic phosphatase activity of *E. coli* suspensions ($2x10^9$ bacteria/ml). pNPP phosphatase activity was measured using a spectrophotometric assay, based on the ability of phosphatases to catalyze the hydrolysis of pNPP to p-nitrophenol, a chromogenic product with absorbance at 420 nm [52]. Initial velocities were calculated as in section 10.

12. Viability

Viability was tested by the capacity of *E. coli* to form colonies (culturability) and their IM integrity (β-galactosidase assay).

Culturability

Bacteria were grown overnight, harvested and resuspended in M9 as explained in section 2. Suspensions of bacteria ($2x10^7$ bacteria/40 μl) were held in the absence of treatments (controls) or were exposed to MST7, MST17 or MEL for 1 or 20 min at 20°C. Afterwards, suspensions were diluted 1/25,000 and 10 μl aliquots were spotted on LB agar plates for overnight culture at 37°C. Colony formed units (CFU) were counted manually and expressed relative to control values.

β-galactosidase assay

This method was used to assess the IM integrity of *E. coli*. *E. coli* BL21 (DE3) were electroporated with a pGEM3ZF plasmid containing a gene encoding β-galactosidase. Transformed bacteria cultures were grown (37°C, 200 rpm) and β-galactosidase expression was induced by the addition of 1.0 mM IPTG to the culture medium. After induction for 3 h, bacterial suspensions were centrifuged at 2,500 g for 5 min, the supernatant was removed and the pellet was

resuspended at $2x10^9$ bacteria/ml in M9 medium. Centrifugation and washing of the pellet was repeated 3 times.

Transformed bacteria were exposed to the chromogenic lactose analog ONPG (o-nitrophenyl β -D-galactopyranoside) in the absence of any treatment (non-treated), or in the presence of MST7, MST17 or MEL.

Agents that compromise IM integrity would permit ONPG to diffuse into bacterial cytoplasm, where it can be hydrolyzed to ONP (o-nitrophenol) by β-galactosidase activity. Accordingly, the concentration of ONP was followed by measuring the absorbance at 415 nm with 1-min intervals for 60 min at 20°C, using a Bio-Rad 550 plate reader. Data were normalized by subtracting absorbance at t=0. The kinetics of ONP production was determined for each treatment.

13. Data analysis

Statistical significance was determined using one-way Analysis of Variance followed by a Tukey Multiple Comparison Test. A p value <0.05 was considered significant. Numbers of determinations (n) from independent preparations (N) are indicated. In the experiments using Caco2 cells, each filter containing polarized monolayers was considered an independent preparation. In experiments using rat intestinal segments, only one segment was excised from each rat. Each segment was considered an independent preparation.

RESULTS

Experiments were performed using suspensions of *E. coli* (PART 1), OMVs (PART 2), Caco-2 cells (PART 3) or intestinal rat segments (PART 4). In these systems, regulation of [ATPe] may depend on the dynamic balance between the rates of ATP release and ATPe hydrolysis. The relative importance of both processes can be assessed by measuring the kinetics of ATPe accumulation (denoted as ATPe kinetics) and ATPase activity.

1. *E. coli*

ATPase activity

Bacterial suspensions were exposed to [γ-^{32}P]ATP at various ATP concentrations (100-1,000 nM), and the time course of [^{32}P]Pi accumulation released from [γ-^{32}P]ATP was determined (Figure 1A). The experimental design for assessing ATPase activity of the periplasm lies on the fact that ATPe is permeable to the OM, but not the IM [4,5]. The initial rate values of [^{32}P]Pi production were used to calculate ATPase activity for each ATPe concentration. ATPase activity followed a linear function with ATPe concentrations (Figure 1B), with slope of the curve (K_{ATP}) amounting to 0.04 min^{-1} per 10^{10} bacteria. Spontaneous ATPe hydrolysis in the absence of bacteria was negligible (inset Figure 1A).

Phosphatase activity

At neutral pH, *E. coli* may exhibit periplasmic ATPase activity by 5'-nucleotidase and alkaline phosphatase. If the latter were active under the experimental conditions, then it should be kinetically inhibited by Pi, and activated at alkaline pH [53,17,8].

Accordingly, we assessed and compared ATPase activity for bacteria suspended in M9 medium, which contains phosphate, with that in Hepes medium, which lacked phosphate. Bacterial suspensions were grown in LB broth (see M&M section 2). They were then collected and resuspended in either M9 or Hepes media. Experiments were run at low [ATPe] (600 nM, Figure 2A) or high [ATPe] (500 µM, Figure 2B), the latter a measure of apparent maximal ATPase activity (Vi). ATPase activities in Hepes medium were 3.3-fold (600 nM ATPe) and 16-fold (500 µM ATPe) higher than those in M9 medium (Figure 2 C-D). Vi was 3.27 ± 1.70 nmol/(10^{10} bacteria min) in Hepes medium and 0.24 ± 0.07 nmol/(10^{10} bacteria min) in M9 medium (Figure 2D).

As a further test for the inhibitory effect of Pi on ATPase activity of alkaline phosphatase, we incubated bacteria in Hepes medium containing the same Pi concentration as in M9 medium. Results showed that, under this condition, ^{32}Pi production at 600 nM ATP was similar to that of M9 medium (Figure 2E). Moreover, while in M9 medium ATPase activity –due to 5'-nucleotidase activity- at pH=9 was roughly similar than at pH=7, in Hepes medium ATPase activity was almost 2-fold higher at pH=9 than at pH=7.

Finally, we tested the capacity of bacterial suspensions to hydrolyze pNPP, a chromogenic product that acts as a substrate for phosphatases, but not for 5'-nucleotidase. As shown in Supplementary Figure 3, phosphatase activity was detected both in M9 and Hepes media. At alkaline pH, phosphatase activity was 2.14 fold higher in the absence of Pi (i.e., Hepes medium), than in its presence (M9 medium).

Effect of AMP-CPP on ATPase activity

AMP-CPP, a non hydrolizable ATP analog, was used as a potential inhibitor of ATPase activity. AMP-CPP is expected to permeate the OM since it is structurally similar to ATP but smaller than the 600-700 Da cut-off size for the permeability of main *E. coli* porins [54]. Bacterial suspensions were exposed to 600 nM ATPe both in Hepes and M9 media (Figure 3A). In media with or without AMP-CPP, ATPase activity in the presence of Hepes medium was higher than that in M9 medium. With 100 µM AMP-CPP, ATPase activity was reduced by approx. 60% (Hepes medium) and 82% (M9 medium) (Figure 3B).

ATPe uptake and ATPase activity

Results above showed that exogenous ATP can be hydrolyzed by *E. coli*. Since enzymes promoting ATPe hydrolysis are located in the periplasm, we checked whether ATPe can be incorporated into bacteria. Aliquots of *E. coli* suspensions were incubated with 1 µM [γ-^{32}P]ATP for 2 or 30 min in M9 medium, after which they were diluted and centrifuged to obtain a pellet. This pellet was then used to determine both the total amount of radioactivity incorporated and, in separate samples, the proportion of this radioactivity due to either [γ-^{32}P]ATP or [γ-^{32}P]Pi contents.

Since M9 has milimolar concentrations of Pi, any nM [γ-^{32}P]Pi accumulated in the extracellular medium will be highly diluted in unlabeled Pi, making direct [γ-^{32}P]Pi uptake into the periplasm negligible. In the bacterial pellet [γ-^{32}P]ATP and [γ-^{32}P]Pi were 1.5- and 2-fold higher at 30 min than at 2 min (Figure 1C), suggesting [γ-^{32}P]-ATP uptake into the periplasm, with subsequent release of [γ-^{32}P]Pi.

For each incubation time, the relative proportion of [γ-^{32}P]Pi, with respect to [γ-

^{32}P]ATP was similar. Total radioactivity of the pellets was not significantly different from the sum of the radioactivity obtained with [γ-^{32}P]Pi + [γ-^{32}P]ATP (Supplementary Figure 4).

ATPe kinetics

In Figure 4A-B, ATPe kinetics from *E. coli* is shown, which depends on both the rates of ATP release (promoting an increase in [ATPe]) and ATPe hydrolysis (promoting a decrease in [ATPe]).

In the absence of stimuli [ATPe] remained steady at 24 ± 3 μM/(10^{10} bacteria).

ATP release was then stimulated by adding MST7 and MEL. These amphipatic peptides can act as permeabilizing agents, compromising bacterial integrity to different extents. Thus, in principle, peptides may trigger ATP release by lytic and non lytic mechanisms. With 10 μM MST7 an acute 3-fold increase in [ATPe] was observed, followed by a slower increase phase. Ten μM MST17, an inactive analog of MST7, produced no effect (Figure 4A).

Both 3 μM and 30 μM MEL (denoted as MEL3 and MEL30 respectively) caused acute ATP releases of different magnitudes. Under MEL3 a 1.4 fold-increase in [ATPe] was observed within 1 min, which remained constant thereafter. On the other hand, MEL30 produced a fast 5 fold-increase in [ATPe] within 1 min, followed by a slower increase phase (Figure 4B). Values of ΔATP_{20}, i.e., values of [ATPe] attained at 20 min post-stimulus for each treatment, are shown as insets of Figures 4A and B.

To illustrate the transient nature of ATP release, Figure 4C shows results obtained by taking the first derivative of ATPe kinetics from Figures 4A-B. In this way the instantaneous changes of [ATPe], an indicator of bacterial ATP permeability (P_{ATP}) could be observed. Both, for MST7 and MEL30, an acute steep increment of P_{ATP}, amounting to 53 (MST7) and 155 (MEL30) μM ATP/(10^{10} bacteria min) was followed by a slower exponential decay.

Intracellular ATP content (ATPi) amounted to 296 ± 78 μM ATP/(10^{10} bacteria). This means that ΔATP_{20} values (i.e. the increase in [ATPe] at 20 min post-stimulus) for MST7, MEL3, and MEL30 represented 22.3%, 5.5% and 87.4% of ATPi, respectively.

Viability

The observed MEL- and MST7- dependent ATPe kinetics in Figure 4 could be induced by lytic and/or non lytic release of ATPi. Therefore, we analyzed the effects of these peptides on the ability of bacteria to form colony units (CFU) and the IM integrity. The latter was measured in transformed *E. coli* BL21 expressing β-galactosidase, in the presence of ONPG.

Formation of colonies on a plate (denoted as culturability) does not necessarily reveal the viability of bacteria under assay conditions but rather tells that there were bacteria in the sample that, after the different treatments, were able to grow and divide.

MST7 and MEL3 decreased CFU formation by approx. 30% (Supplementary Figure 5). In both cases the effects were acute, since for each peptide, CFU values after 1 min exposure were not statistically different from those obtained after 20 min. MST17 did not change CFU values. Exposure to MEL30, on the other hand, decreased CFU values by 57% and 79% at 1 and 20 min, respectively (Supplementary Figure 5A).

The β-galactosidase assay showed similar activity values for control and MST17 treated samples. While exposure to MST7 or MEL3 caused no changes in β-galactosidase activity, under MEL30 a different pattern was observed. In this case low increments in activity at relatively low incubation times (0-5 min) were followed by strong increases, of about 5.6-fold, at later times (5-20 min) (Supplementary Figure 5B-C). Thus, except for MEL30, the observed decrease of culturability observed using MST7 and 3 μM MEL occurs without viability (as assayed by β-galactosidase activity) being compromised.

2. Outer membrane vesicles (OMVs)

OMVs originate from *E. coli* under culture. Following purification, OMVs were detected by electron microscopy as spherical vesicles with diameters ranging from 50 to 200 nm, surrounding an electrodense center (Figure 5A), as previously described [55,56].

TLC analysis showed that OMVs were composed by LPS, PE and CL (Figure 5B), the main phospholipids classes present in the OM of Gram-negative bacteria.

Since during formation OMVs encapsulate portions of the bacterial periplasm

with soluble proteins, they might exhibit ATPase activity due to –originally periplasmic- nucleotidases and phosphatases. Moreover, if significant ATP amounts were present in the vesicles' lumen, then this pool might be released by MEL and MST7 exposure. Accordingly, as with *E. coli*, ATPase activity and ATPe kinetics of OMVs were studied.

ATPase activity

ATPase activity of OMVs was obtained by real-time luminometry after addition of ATP. Figure 5C shows a steady pre-stimulus ATPe level, followed by an acute increase when ATP was added. The subsequent kinetics of [ATPe] decrease could be used to estimate ATPase activity (see section 10.3 in M&M) at each [ATPe], from which a substrate curve could be built (Figure 5D). Such a curve showed ATPase activity to increase with [ATPe]. Moreover, a determination of ATPase activity using [γ^{32}P]-ATP at a single [ATPe] provided similar results (See Figure 5D and Supplementary Figure 6).

ATPe kinetics

In the absence of stimuli, [ATPe] of OMVs amounted to 13 ± 5 nM/(µg protein). Under MST7 exposure, a 3 fold-increase in [ATPe] was observed within 1 min, followed by a slower increase phase. Exposure to MEL30 caused an acute 7 fold-increase in [ATPe], followed by a continuous increasing phase (Figure 6). At more prolonged exposure times, [ATPe] decreased due to ATPase activity (Supplementary Figure 7). Values of ΔATP_{20} showed a 4-fold higher [ATPe] for MEL30 than for MST7 (inset of Figure 6).

OMVs is a much simpler system than *E. coli*. Vesicles have a single internal compartment containing ATP, and mechanisms enabling ATP synthesis do not exist. On the other hand, periplasmic ATP of *E. coli* can be influenced by cytosolic ATP (produced by an ATP synthase) as well as ATPe. Despite these differences, we tested whether ATPe kinetics of OMVs may mimic that of bacteria.

Accordingly, ATPe kinetics of OMVs and *E. coli* exposed to MST7 and MEL30 were compared by means of a correlation plot. Results showed a linear relationship for [ATPe] values of *E. coli* and OMVs for at least 5 min, although at later times this linearity was lost (Supplementary Figure 8 A-B).

3. Caco-2 cells

Results of Part 1 showed that *E. coli* is capable of ATPe uptake and hydrolysis and in the presence of amphipatic peptides, release of intracellular ATP. Since *in vivo E. coli* may metabolically interact with intestinal epithelial cells of the human host, we evaluated the effect of *E. coli* on ATPe kinetics of Caco-2 cells, a model of epithelial enterocytes, and the potential effect of *E. coli* on this kinetics.

Caco-2 cells were grown as a polarized epithelial cell monolayer. ATPe kinetics was quantified on the apical side using real time luminometry (Supplementary Figure 2).

In the absence of bacteria, Caco-2 cells showed a basal rate of ATPe decrease amounting to 0.03 ± 0.003 nM/min. Addition of exogenous ATP (1.4 -7 µM) led to an acute [ATPe] increase, followed by a decay phase (Figure 7A). The resulting decay kinetics were used to estimate ATPase activity.. This was a linear function of [ATPe] over an ample nM-µM range (Figure 7B), with the slope of the curve (K_{ATP}) amounting to 0.023 min^{-1} for approx. $5x10^5$ cells per well. Rates of ATPe hydrolysis by assessing ^{32}P-Pi production provided similar results (Supplementary Figure 9).

Next, we determined the effect of *E. coli* and of 3V on ATPe kinetics of Caco-2 cells. 3V is an adrenergic cocktail that can trigger ATP release via elevation of cAMP [38,50,57]. Experiments were run in the absence and presence of carbenoxolone (CBX), a generic blocker of ATP release of most eukaryotic cells [46,32]. Accordingly, stimuli were added to the apical medium and ATPe kinetics of Caco-2 cells was determined.

In the absence of stimuli [ATPe] of Caco2 cells amounted to 123 ± 5 nM (Figures 7C and D). Addition of 3V (Figure 7C) or *E. coli* ($2x10^7$ bacteria, Figure 7D) led to a 6 fold-increase in [ATPe] within 1 min to a maximum, followed by an acute decrease. These peaks were reduced 58-77% by CBX (inset Figure 7 C-D), though the effect of CBX on 3V induced ATP release was not significant (p=0.12).

4. Intestinal rat segments

Bacterial suspensions were perfused through the lumen of jejunum rat segments. These conserved the intestinal wall structure and can therefore exhibit smooth muscle contractions that might influence ATP release. Luminal ATP_L was monitored by off-line luminometry.

In the absence of bacteria [ATP_L] remained steady for 90 min at 13 ± 2 nM (N=2, Supplementary Figure 10).

Then ATP_L was measured in perfusate samples in the absence of bacteria during 30 min at 10 min intervals. Subsequently, the Ringer solution was replaced by a bacterial suspension containing $5x10^8$ bacteria /mL and ATP_L was measured every 10 min during the next 60 min (Figure 8A). Compared with basal pre-stimulated ATP_L values, *E. coli* suspensions induced a 2-fold increase of ATP_L maximal value determined within the 30 min exposure to bacterial perfusion ($p<0.05$, Figure 8B, N=4). After 40 min, ATP_L decreased to basal pre-stimulated levels (Figure 8A).

Next, we checked whether the observed increased in ATP_L was caused by the ATPe content of the bacterial suspension. Thus, bacterial suspensions were centrifuged, and the supernatant was collected. Then, intestinal segments were perfused with Ringer solution, followed by the bacterial supernatant and finally the bacterial suspension (Figure 8C). Results show that maximal ATP_L levels, compared to basal values, were 3-fold and 5-fold higher with the bacterial supernatant and the bacterial suspension, respectively (Figure 8D). This means that endogenous ATPe of bacteria, as well as bacteria themselves, are causing increases of ATP_L levels.

DISCUSSION

Results of this study show that ATPe regulation in *E. coli* results from a dynamic balance between the rates of ATP release and ATPe hydrolysis. Moreover, we show that OMVs, produced and released by *E. coli* under standard growth conditions, retain key features of the processes mediating ATPe regulation in bacteria. In addition, we found that *E. coli* can strongly enhance ATPe release of Caco-2 cells and intestinal rat segments.

Studies using *E. coli* and OMVs

Addition of exogenous ATP to bacterial suspensions, which should promote ATP transport through OM porins into the periplasm [4,7], led to significant ATPe uptake and hydrolysis.

ATPase activity increased in proportion to [ATPe] over a wide nanomolar range (Figure 1B). A similar pattern was observed in OMVs, which is consistent with these vesicles encapsulating portions of the bacterial periplasm containing functional enzymes [44].

Based on previous reports [5,15] we propose periplasmic 5'nucleotidase and alkaline phosphatase to be responsible for the observed ATPe hydrolysis at neutral pH. To further corroborate the functional presence of these enzymes, we evaluated the effect of medium Pi. 5'nucleotidases from bacteria and various vertebrate species do not show product inhibition [58,15]. Regarding alkaline phosphatase, although a transcriptional downregulation of the enzyme in the presence of Pi was postulated, this mechanism was impeded under the high Pi culture conditions. Nevertheless, several reports showed that Pi can kinetically inhibit alkaline phosphatase activity of *E. coli* [18,59].

Thus, in addition to experiments using M9 medium (containing mM Pi), we also evaluated ATPase activity in media lacking phosphate (i.e., Hepes Medium), a condition where a strong increase of ATPe hydrolysis was found. Two components of ATPe hydrolysis were observed, one which is relatively insensitive to Pi, consistent with 5'nucleotidase activity, and a second component which was kinetically inhibited by Pi, and activated at alkaline pH, consistent with alkaline phosphatase.

Since in both, *E. coli* and OMVs, ATPe hydrolysis was a linear function of [ATPe], any increase of the nucleotide will at least be partially downregulated by increases of periplasmic (bacteria) or intravesicular (OMV) ATPase activity..

Having shown that periplasmic ATPase activity is active under the experimental conditions, we turned our attention to bacterial ATP release. This was estimated by studying ATPe kinetics in the absence and presence of two amphipatic peptides, MST7 and MEL. In unstimulated conditions a stable nanomolar level

of ATPe was observed (Figures 4A and B). This is compatible with a potential low rate of ATP release being counterbalanced by periplasmic ATPase activity.
In line with this idea, other authors found no ATP secretion of *E. coli* in the absence of stimuli [58]. Moreover, when expression of periplasmic 5'-nucleotidase and alkaline phosphatase of *E. coli* was blocked, ATP release could be observed in the absence of stimulus [5], a process that would lead to [ATPe] accumulation.
Basal [ATPe] was challenged when *E. coli* were perturbed by exposure to MST7 and MEL. Addition of the peptides caused a 3-fold (MST7) and 7-fold (MEL30) increase of [ATPe] within 1 min, with the amplitude of ATPe response at 20 min post-stimulus ranging from 66 μM/(10^{10} bacteria) (MST7) to 259 μM/(10^{10} bacteria) (MEL30).. Changes in [ATPe] were achieved by triggering a strong initial rate of ATP release (denoted as P_{ATP} in Figure 4C) under MST7 (≈53 μM/min) and MEL30 (≈155 μM/min). These rates were approx. 30-fold higher than ATPase activities under the same conditions. Thus the acute phase of ATPe kinetics mostly reflected the kinetics of ATP release. At later times, however, the rate of [ATPe] increase slowed down rapidly. While with MST7 a decrease of [ATPe] was not observed during 20 min exposure, with MEL30 [ATPe] started to decrease at approx. 12 min post-stimulus, an indication that ATP release is inactivated with time while ATPase activity progressively begun to govern ATPe kinetics.
Overall these results show that *E. coli* exhibit basal ATPe levels, which strongly increased when bacteria were challenged by permeabilizers.
E. coli-derived ATPe may stimulate biofilm formation and adherence [60], promote bacterial growth, or even act as a quorum sensing signal [3].
Since bacterial ATP release can be caused by lytic and non lytic mechanisms, two aspects of viability were analyzed, i.e., the capacity of bacteria to form colonies on solid agar plates (CFU) and the IM integrity, estimated by β-galactosidase activity.
Within 1 min, 10 μM MST7 and 3 μM MEL decreased CFU formation by approx. 30% (Supplementary Figure 5A), with no changes thereafter. Exposure to 30 μM MEL produced a stronger decrease of CFU.. β-galactosidase activity showed no changes with 10 μM MST7 or 3 μM MEL, while 30 μM MEL produced a different pattern. In this case low increments at low incubation times

(0-5 min) were followed by strong increases at later times (5-20 min) (Supplementary Figure 5B). Thus MEL30, but not MST7, compromised the IM. In agreement with these findings, Katsu et al. (1990) showed that MST perturbed the IM of *E. coli* only when the OM was previously disrupted [23]. Instead, MEL was able to disrupt both membranes in a dynamic fashion; it can assemble to form transient pores in the OM and then translocate to the IM, inducing the leakage of cytoplasmic contents [9].

Therefore, ATP efflux induced by MST7 was compatible with changes only in the permeability of the OM, suggesting ATP release from the periplasm, even though subsequent culture generated a decrease of culturability.

Under MEL30, on the other hand, the acute phase of [ATPe] increase would be mostly non lytic, followed by a later increase phase where the IM is compromised, a condition where the ATPcyt content can be released, thus leading to the observed high amplitude of ATPe kinetics. Accordingly, after 20 min of MEL30 exposure 87% of intracellular ATP was released by a combination of lytic and non lytic mechanisms. The late decrease of [ATPe] could be due to ATPase activity of periplasmic and cytoplasmic nucleotidases and phosphatases.

Thus, ATP is released by a combination of lytic and non lytic mechanisms. Under partial bacteriolysis, dying bacteria might release ATP and other nucleotides, which can be taken up and metabolized by viable bacteria.

ATPe kinetics of OMVs was qualitatively similar to that obtained with *E. coli;* [ATPe] remained steady in the absence of stimuli, and acutely increase in the presence of the peptides.

Values of [ATPe] at each time point from OMVs were compared with similar values from *E. coli*. This correlation plot (Supplementary Figure 8A-B) showed a roughly linear relationship for [ATPe] values of *E. coli* and OMVs for at least 5 min (the acute phase), although a later times this linearity was lost. This can be due to several reasons. First, OMVs are smaller than *E. coli* and as such represent a simpler system where, unlike whole bacteria, ATPe regulation can be studied in the absence of cytoplasmic contents, that is, with no synthesis or release of ATPcyt. In addition, several authors reported that some OM proteins can be disproportionately enriched in OMVs, whereas others can be excluded,

so that an altered capacity for the proteins involved in ATPe regulation may occur.

OMVs may contain DNA, and proteins exhibiting various biological activities [44], such as proteases, peptidases and β-lactamases [61]..

In this context we show that OMVs contain intravesicular ATP, and that –similarly to bacteria- this nucleotide can be released when vesicles are exposed to permeabilizers. This is important inasmuch as OMVs were shown to lyse when exposed to external stimuli [62] or open transiently [63].

Bacteria, and therefore, OMVs, lack purinergic receptors (for extracellular di- and trinucleotides), so that signalling via these receptors is assumed to be absent in *E. coli* and other microorganisms [3]. Although speculative, OMVs, acting as delivery vesicles containing ATP and ATPases, might modulate the purinergic signaling system of the host

Figure 9 provides a qualitative model of ATPe regulation of *E. coli* and their OMVs. Under culture conditions, OMVs are formed from *E. coli*. ATP can be present in the cytosol, the periplasm, the extracellular space or the lumen of OMVs. In both, OMVs or bacteria, regulation of ATPe depends on the dynamic balance between the rates of ATP hydrolysis, facilitated by nucleotidases/phosphatases of the periplasm (*E. coli*) or vesicular lumen (OMVs) and of ATP release. Permeabilizers can act on the OM alone (MST7) or both on the outer and inner membrane (MEL).

Effect of *E. coli* on ATPe kinetics of Caco-2 cells

Caco-2 cells have been previously shown to release ATP when exposed to hypotonicity [64]. Our results also showed regulated ATP release, in this case when cells were exposed apically to an adrenergic cocktail containing isoproterenol. This was not unexpected, since in these cells isoproterenol was shown to increase cAMP and Ca^{2+} [65,66], two well known second messengers triggering ATP release in different cell types [38,67,68] see Lazarowski 2012 [69]. ATPe concentration showed a fast steep increase to a maximum, followed by a slower ATPe decay (Figure 7A). The latter is indicative of a high rate of extracellular ATPase activity, which could be corroborated by measuring ATPe

consumption and ^{32}P-Pi production under exposure to ATP (Supplementary Figure 9).

Thus, aliquots of *E. coli* were added to the apical side of Caco-2 cells, leading to a strong [ATPe] increase to a maximum, followed by an acute decrease (Figure 7D).

In Caco-2 cells, the initial rate of ATP release induced by *E. coli* (derived from data of Figure 7D), was about 30-fold higher than the rate of ATPe hydrolysis (Figure 7B) of these cells at similar ATPe levels. Therefore, during this brief phase of ATPe accumulation, quantified as ΔATP_1 (inset of Figure 7D) bacterial-induced ATPe kinetics was mainly governed by Caco-2 apical release of intracellular ATP. At later times, however, [ATPe] decreased non linearly, implying that ATPe release is downregulated while ATPe hydrolysis begun to dominate ATPe kinetics. Similarly, enteropathogenic *E. coli* induced ATP release of TC7 epithelial cells, although the experimental setup did not allow to distinguish the apical and the basolateral components of ATP release [70].

We wondered what the relative contribution of bacteria and Caco2-cells was to this late ATPe decay kinetics? Under the experimental conditions (Supplementary Figure 2), with about $5x10^5$ Caco-2 cells exposed to $2x10^7$ *E. coli*, the corresponding values of K_{ATP} (which estimates the rate of ATPe hydrolysis, Figure 7B) would be $3x10^{-2}$ min^{-1} (Caco-2) and $8x10^{-5}$ min^{-1} (*E. coli*). Thus, the capacity to hydrolyze ATPe was about 300 times higher for Caco-2 cells than for bacteria. This is in agreement with Caco-2 cells exhibiting activities of ectonucleotidases and ectophosphatases, and their derived exosomes exhibiting strong ectoATPase activity [65,66]. Thus, the observed ATPe decay kinetics of Figure 7D was governed by extracellular ATPase activity of Caco-2 cells, with no contribution from *E. coli*..

As a complementary proof for the effect of *E. coli* on intestinal cells, we used rat jejunum segments.

Unlike Caco-2 cells, which represent an *in vitro* model of the enterocytes lining the intestinal cavity, rat intestinal segments conserve the complete intestinal wall structure. [ATPe] significantly increased short after *E. coli* injection in rat jejunum segments (Figure 8A). Similarly, injection of the pathogenic Gram(-) *Shigella flexneri* in rabbit ileum segments caused luminal ATP release [70].

Interestingly, the observed ATP_L increase was not only due to intestinal ATP release, but also to the endogenous ATPe of bacteria (Figure 8C).

The above considerations imply that *E. coli* are strong inducers of ATPe kinetics of intestinal cells. On the other hand, *E. coli* and their OMVs might release low micromolar ATPe under situations compromising their integrity (Figures 4 and 6). This could activate P2Y2 receptors (EC_{50} for ATP ≈ 80 nM, [68], which are functional at the apical domain of Caco-2 cells [71,72]. Activation of $P2Y_{2,4,6}$ receptors of intestinal cells and various intestinal cell lines has been shown to regulate transepithelial ionic transport [73,74]..

In short, results of this study show that *E. coli* can trigger apical ATP release from an intestinal epithelial cell model and rat intestinal segments, and simultaneously take up and hydrolyze submicromolar ATP. ATPe hydrolysis can be further enhanced by ectoATPase activity of Caco-2 cells, and potentially by ATPase activity of OMVs. This is metabolically important since *E. coli* is also permeable to ATPe hydrolysis products such as ADP and AMP [4].

Given that the intestinal mucosa is a purine-limited environment [75], ATPe metabolism by *E. coli* could be part of a nutritional program whereby successful colonization of the colon by at least five different –non pathogenic- *E. coli* strains depend upon competition for nutrients with a dense and diverse microbiota, with up to 1,000 different commensal species [76].

Alternatively, ATP release of bacteria may supply energy and hence facilitate the formation and survival of bacterial communities [3].

Future studies would allow to discern the extent to which bacteria and OMVs can modulate nucleotide dependent cellular and systemic responses of the host, such as inflammation, proliferation, vasodilation, apoptosis and cell volume.

REFERENCES

1. Lasko DR, Wang DIC. On-line monitoring of intracellular ATP concentration in Escherichia coli fermentations. Biotechnology and Bioengineering. 1996;52(3):364–72.
2. Schneider DA, Gourse RL. Relationship between growth rate and ATP concentration in escherichia coli: A bioassay for available cellular ATP. Journal of Biological Chemistry. 2004;279(9):8262–8.
3. Mempin R, Tran H, Chen C, Gong H, Kim Ho K, Lu S. Release of extracellular ATP by bacteria during growth. BMC microbiology [Internet]. 2013;13:301. Available from: http://www.biomedcentral.com/1471-2180/13/301\nhttp://www.biomedcentral.com/content/pdf/1471-2180-13-301.pdf
4. Watanabe K, Tomioka S, Tanimura K, Oku H, Isoi K. Uptake of AMP, ADP, and ATP in Escherichia coli W. Bioscience, biotechnology, and biochemistry [Internet]. 2011;75(1):7–12. Available from: http://www.ncbi.nlm.nih.gov/pubmed/21228488
5. Kakehi M, Usuda Y, Tabira Y, Sugimoto S. Complete deficiency of 5′-nucleotidase activity in Escherichia coli leads to loss of growth on purine nucleotides but not of their excretion. Journal of Molecular Microbiology and Biotechnology. 2007;13(1-3):96–104.
6. Heller KB, Wilson TH. Selectivity of the *Escherichia coli* outer membrane porins ompC and ompF. FEBs Letters. 1981;129(2):253–5.
7. Samartzidou H, Delcour AH. Distinct sensitivities of OmpF and PhoE porins to charged modulators. FEBS Letters. 1999;444(1):65–70.
8. Benz R, Schmid A, Nakae T, Vos-Scheperkeuter GH. Pore formation by LamB of Escherichia coli in lipid bilayer membranes. Journal of Bacteriology. 1986;165(3):978–86.
9. Gee ML, Burton M, Grevis-James A, Hossain MA, McArthur S, Palombo EA, et al. Imaging the action of antimicrobial peptides on living bacterial cells. Scientific reports [Internet]. 2013;3:1557. Available from: http://www.nature.com/srep/2013/130327/srep01557/fig_tab/srep01557_F6.html
10. Mathis RR, Brown OR. Biochimica et Biophysica Acta, 440 (1976) 723-732 © Elsevier Scientific Publishing Company, Amsterdam - Printed in the Netherlands. 1976;440:723–32.
11. Soini J, Falschlehner C, Mayer C, Böhm D, Weinel S, Panula J, et al. Transient increase of ATP as a response to temperature up-shift in Escherichia coli. Microbial cell factories. 2005;4:9.
12. Ivanova EP, Alexeeva Y V., Pham DK, Wright JP, Nicolau D V. ATP level variations in heterotrophic bacteria during attachment on hydrophilic and hydrophobic surfaces. International Microbiology. 2006;9(1):37–46.
13. Weiss B. YjjG, a dUMP phosphatase, is critical for thymine utilization by Escherichia coli K-12. Journal of Bacteriology. 2007;189(5):2186–9.
14. Cowman A, Beacham IR. Molecular cloning of the gene (ush) from Escherichia coli specifying periplasmic UDP-sugar hydrolase (5'-nucleotidase). Gene [Internet]. 1980;12(3-4):281–6. Available from: http://eutils.ncbi.nlm.nih.gov/entrez/eutils/elink.fcgi?dbfrom=pubmed&id=6265322&retmode=ref&cmd=prlinks\npapers3://publication/uuid/2A610A3B-A092-4C14-B75B-0BE27C9BC0B8

15. Sträter N. Ecto-5′-nucleotidase: Structure function relationships. Purinergic Signalling. 2006;2(2):343–50.
16. Thaller, MC, Schipa S, Bonci A, Cresti S, Rossolini GM. Identification of the gene (*aphA*) encoding the class B acid phosphatase/phosphotransferase of Escherichia coli MG1655 and characterization of its product. FEMS Microbiology Letters. 1997; 146: 191-8.
17. Torriani A, Rothman F. Mutants of Escherichia Coli Constitutive for Alkaline Phosphatase1. Journal of Bacteriology. 1961;81(5):835–6.
18. Chaidaroglou A, Brezinski DJ, Middleton SA, Kantrowitz ER. Function of Arginine- 166 in the Active Site of Escherichia coli Alkaline Phosphatase. Biochemistry 1988, 27, 8338-8343.
19. Rao NN, Wang E, Yashphe J, Torriani A. Nucleotide pool in pho regulon mutants and alkaline phosphatase synthesis in Escherichia coli. Journal of Bacteriology. 1986;166(1):205–11.
20. Berrier C, Coulombe A, Szabo I, Zoratti M, Ghazi A. Gadolinium ion inhibits loss of metabolites induced by osmotic shock and large stretch-activated channels in bacteria. European Journal of Biochemistry. 1992;206(2):559–65.
21. Weigel NS, Powers DA and Roseman S. Sugar Transport by the Bacterial Phosphotransferase System. The Journal of Biological Chemistry. 1982; 257 (23): 14499-14509.
22. Katsu T, Kuroko M, Morikawa T, Sanchika K, Fujita Y, Yamamura H, et al. Mechanism of membrane damage induced by the amphipathic peptides gramicidin S and melittin. BBA - Biomembranes. 1989;983(2):135–41.
23. Katsu T, Kuroko M, Morikawa T, Sanchika K, Yamanaka H, Shinoda S, et al. Interaction of wasp v e n o m mastoparan with biomembranes. 1990;1027:185–90.
24. Dempsey CE. The actions of melittin on membranes. Biochimica et Biophysica Acta - Reviews on Biomembranes. 1990;1031(2):143–61.
25. Oh JT, Cajal Y, Skowronska EM, Belkin S, Chen J, Van Dyk TK, et al. Cationic peptide antimicrobials induce selective transcription of micF and osmY in Escherichia coli. Biochimica et Biophysica Acta - Biomembranes. 2000;1463(1):43–54.
26. Ulvatne H, Karoliussen S, Stiberg T, Rekdal Ø, Svendsen JS. JAC against Escherichia coli. Antimicrobial Agents and Chemotherapy. 2001;(203):203–8.
27. Sugama J, Ohkubo S, Atsumi M, Nakahata N. Mastoparan Changes the Cellular Localization of G ⎵ q / 11 and G through Its Binding to Ganglioside in Lipid Rafts. 2005;68(5):1466–74.
28. Lin C, Tzen JTC, Shyu C, Yang MJ, Tu W. Peptides Structural and biological characterization of mastoparans in the venom of Vespa species in Taiwan. Peptides [Internet]. Elsevier Inc.; 2011;32(10):2027–36. Available from: http://dx.doi.org/10.1016/j.peptides.2011.08.015
29. Walrant A, Correia I, Jiao CY, Lequin O, Bent EH, Goasdoué N, et al. Different membrane behaviour and cellular uptake of three basic arginine-rich peptides. Biochimica et Biophysica Acta - Biomembranes [Internet]. Elsevier B.V.; 2011;1808(1):382–93. Available from: http://dx.doi.org/10.1016/j.bbamem.2010.09.009
30. Da Silva AVR, De Souza BM, Dos Santos Cabrera MP, Dias NB, Gomes

PC, Neto JR, et al. The effects of the C-terminal amidation of mastoparans on their biological actions and interactions with membrane-mimetic systems. Biochimica et Biophysica Acta - Biomembranes [Internet]. Elsevier B.V.; 2014;1838(10):2357–68. Available from: http://dx.doi.org/10.1016/j.bbamem.2014.06.012
31. Amro N a, Amro N a, Kotra LP, Kotra LP, Wadu-Mesthrige K, Wadu-Mesthrige K, et al. High-resolution atomic force microscopy studies of the Escherichia coli outer membrane: Structural basis for permeability. Langmuir. 2000;16(15):2789–96.
32. Zhang Y, Phillips GJ, Yeung ES. Real-time monitoring of single bacterium lysis and leakage events by chemiluminescence microscopy. Analytical Chemistry. 2007;79(14):5372–81.
33. López-García B, Gandía M, Muñoz A, Carmona L, Marcos JF. A genomic approach highlights common and diverse effects and determinants of susceptibility on the yeast Saccharomyces cerevisiae exposed to distinct antimicrobial peptides. BMC Microbiology [Internet]. 2010;10(1):289. Available from: http://www.biomedcentral.com/1471-2180/10/289
34. Laverty G, Gorman SP, Gilmore BF. The potential of antimicrobial peptides as biocides. International Journal of Molecular Sciences. 2011;12(10):6566–96.
35. Nakao S, Komagoe K, Inoue T, Katsu T. Comparative study of the membrane-permeabilizing activities of mastoparans and related histamine-releasing agents in bacteria, erythrocytes, and mast cells. Biochimica et Biophysica Acta - Biomembranes [Internet]. Elsevier B.V.; 2011;1808(1):490–7. Available from: http://dx.doi.org/10.1016/j.bbamem.2010.10.007
36. Oren Z, Shai Y. Selective lysis of bacteria but not mammalian cells by diastereomers of melittin: Structure-function study. Biochemistry. 1997;36(7):1826–35.
37. Pandey BK, Ahmad A, Asthana N, Azmi S, Srivastava RM, Srivastava S, et al. Cell-selective lysis by novel analogues of melittin against human red blood cells and escherichia coli. Biochemistry. 2010;49(36):7920–9.
38. Leal Denis MF, Incicco JJ, Espelt MV, Verstraeten S V., Pignataro OP, Lazarowski ER, et al. Kinetics of extracellular ATP in mastoparan 7-activated human erythrocytes. Biochimica et Biophysica Acta - General Subjects [Internet]. Elsevier B.V.; 2013;1830(10):4692–707. Available from: http://dx.doi.org/10.1016/j.bbagen.2013.05.033
39. Leal Denis MF, Alvarez HA, Lauri N, Alvarez CL, Chara O, Schwarzbaum PJ. Dynamic Regulation of Cell Volume and Extracellular ATP of Human Erythrocytes. Plos One [Internet]. 2016;11(6):e0158305. Available from: http://dx.plos.org/10.1371/journal.pone.0158305
40. Kuroda A, Kornberg A. Polyphosphate kinase as a nucleoside diphosphate kinase in *Escherichia coli* and *Pseudomonas aeruginosa*. Pnas. 1997;94(2):439–42.
41. Legendre L, Yueh YG, Crain R, Haddock N, Heinstein PF, Low PS. Phospholipase C activation during elicitation of the oxidative burst in cultured plant cells. Journal of Biological Chemistry. 1993;268(33):24559–63.
42. Amano A, Takeuchi H, Furuta N. Outer membrane vesicles function as offensive weapons in host-parasite interactions. Microbes and Infection

[Internet]. Elsevier Masson SAS; 2010;12(11):791–8. Available from: http://dx.doi.org/10.1016/j.micinf.2010.05.008
43. Kuehn MJ, Kesty NC. Bacterial outer membrane vesicles and the host – pathogen interaction. Genes & Development. 2005; 2645–55.
44. Kulp A, Kuehn MJ. Biological functions and biogenesis of secreted bacterial outer membrane vesicles. Annual review of microbiology [Internet]. NIH Public Access; 2010 [cited 2016 Jul 4];64:163–84. Available from: http://www.ncbi.nlm.nih.gov/pubmed/20825345
45. Kadurugamuwa JL, Beveridge TJ . Bacteriolytic effect of Membrane Vesicles from *Pseudomonas aeruginosa* on other bacteria including Pathogens: Conceptually New Antibiotics. Journal of Bacteriology. 1996, 178 (10): 2767-74.
46. Li Z, Clarke AJ, Beveridge TJ, Acteriol JB. A Major Autolysin of Pseudomonas aeruginosa : Subcellular Distribution , Potential Role in Cell Growth and Division , and Secretion in Surface Membrane Vesicles Downloaded from http://jb.asm.org/ on December 5 , 2014 by The University of British Columbia . 1996;178(9):2479–88.
47. Herlax V, Henning MF, Bernasconi AM, Goni FM, Bakas L. The lytic mechanism of Escherichia coli α-hemolysin associated to outer membrane vesicles. Health [Internet]. 2010;02(05):484–92. Available from: http://www.scirp.org/journal/PaperInformation.aspx?PaperID=1816&#abstract
48. Folch J, Lees M, Sloane Stanley G. H. A simple method for the isolation and purification of total lipids from animal tissues. Journal of Biological Chemistry. 1957, 226:497-509.
49. Pafundo DE, Chara O, Faillace MP, Krumschnabel G, Schwarzbaum PJ. Kinetics of ATP release and cell volume regulation of hyposmotically challenged goldfish hepatocytes. American journal of physiology Regulatory, integrative and comparative physiology [Internet]. 2008;294(1):R220–33. Available from: http://www.ncbi.nlm.nih.gov/pubmed/17928510
50. Montalbetti N, Leal Denis MF, Pignataros OP, Kobatake E, Lazarowski ER, Schwarzbaum PJ. Homeostasis of extracellular ATP in human erythrocytes. Journal of Biological Chemistry. 2011;286(44):38397–407.
51. Schwarzbaum PJ, Kaufman SB, Rossi RC, Garrahan PJ. An unexpected effect of ATP on the ratio between activity and phosphoenzyme level of Na +/K+-ATPase in steady state. Biochimica et biophysica acta. 1995;1233:33–40.
52. Mackintosh C. Protein Phosphorylation: A Practical Approach, ed HardieD. G. 1993, IRL Press, Oxford, UK. pp 197–230
53. Torriani A. Influence of inorganic phosphate in the formation of phosphatases by Escherichia coli. Biochimica et biophysica acta. 1960;38(1957):460–9.
54. Koebnik R, Locher KP, Van Gelder P. Structure and function of bacterial outer membrane proteins: barrels in a nutshell. Molecular microbiology. 2000;37(2):239–53.
55. Kesty NC, Mason KM, Reedy M, Miller SE, Kuehn MJ. Enterotoxigenic Escherichia coli vesicles target toxin delivery into mammalian cells. The EMBO journal. 2004;23(23):4538–49.

56. Roier S, Zingl FG, Cakar F, Durakovic S, Kohl P, Eichmann TO, et al. A novel mechanism for the biogenesis of outer membrane vesicles in Gram-negative bacteria. Nature communications [Internet]. 2016;7:10515. Available from: http://www.nature.com/doifinder/10.1038/ncomms10515%5Cnhttp://www.ncbi.nlm.nih.gov/pubmed/26806181%5Cnhttp://www.pubmedcentral.nih.gov/articlerender.fcgi?artid=PMC4737802
57. Alvarez CL, Schachter J, de Sá Pinheiro AA, Silva L de S, Verstraeten SV, Persechini PM, et al. Regulation of extracellular ATP in human erythrocytes infected with Plasmodium falciparum. PloS one [Internet]. 2014;9(5):e96216. Available from: http://journals.plos.org/plosone/article?id=10.1371/journal.pone.0096216
58. Zimmermann H. Extracellular ATP and other nucleotides—ubiquitous triggers of intercellular messenger release. Purinergic Signalling. 2016;12(1):25–57.
59. Holtz KM, Kantrowitz ER. The mechanism of the alkaline phosphatase reaction: Insights from NMR, crystallography and site-specific mutagenesis. FEBS Letters. 1999;462(1–2):7–11.
60. Xi C, Wu J. dATP/ATP, a multifunctional nucleotide, stimulates bacterial cell lysis, extracellular DNA release and biofilm development. PLoS ONE. 2010;5(10).
61. Kulkarni HM, Swamy CVB, Jagannadham M V. Molecular characterization and functional analysis of outer membrane vesicles from the Antarctic bacterium Pseudomonas syringae suggest a possible response to environmental conditions. Journal of Proteome Research. 2014;13(3):1345–58.
62. Li Z, Clarke AJ, Beveridge TJ. Gram-Negative Bacteria Produce Membrane Vesicles Which Are Capable of Killing Other Bacteria Gram-Negative Bacteria Produce Membrane Vesicles Which Are Capable of Killing Other Bacteria. Journal of bacteriology. 1998;180(20):5478–83.
63. Renelli M, Matias V, Lo RY, Beveridge TJ. DNA-containing membrane vesicles of Pseudomonas aeruginosa PAO1 and their genetic transformation potential. Microbiology. 2004;150(7):2161–9.
64. Ullrich N, Caplanusi A, Brône B, Hermans D, Larivière E, Nilius B, et al. Stimulation by caveolin-1 of the hypotonicity-induced release of taurine and ATP at basolateral, but not apical, membrane of Caco-2 cells. American journal of physiology Cell physiology [Internet]. 2006;290(5):C1287–96. Available from: http://www.ncbi.nlm.nih.gov/pubmed/16338968
65. Krolczyk AJ, Bear CE, Lai PF, Schimmer BP. Effects of mutations in cAMP-dependent protein kinase on chloride efflux in Caco-2 human colonic carcinoma cells. Journal of cellular physiology. 1995;162(1):64–73.
66. Battistoni A. Escherichia coli. Protein Science. 1996;160(10):287–2127.
67. Lazarowski ER, Sesma JI, Seminario-Vidal L, Kreda SM. Molecular Mechanisms of Purine and Pyrimidine Nucleotide Release [Internet]. 1st ed. Vol. 61, Advances in Pharmacology. Elsevier Inc.; 2011. 221-261 p. Available from: http://dx.doi.org/10.1016/B978-0-12-385526-8.00008-4
68. Lazarowski ER, Boucher RC, Harden TK. Mechanisms of Release of Nucleotides and Integration of Their Action as P2X- and P2Y-Receptor

Activating Molecules. Molecular Pharmacology [Internet]. 2003;64(4):785–95. Available from: http://molpharm.aspetjournals.org
69. Lazarowski ER. Vesicular and conductive mechanisms of nucleotide release. Purinergic Signalling. 2012;8(3):359–73.
70. Puhar A, Tronchère H, Payrastre B, Tran Van Nhieu G, Sansonetti PJ. A Shigella Effector Dampens Inflammation by Regulating Epithelial Release of Danger Signal ATP through Production of the Lipid Mediator PtdIns5P. Immunity. 2013;39(6):1121–31.
71. McAlroy HL, Ahmed S, Day SM, Baines DL, Wong HY, Yip CY, et al. Multiple P2Y receptor subtypes in the apical membranes of polarized epithelial cells. BrJ Pharmacol. 2000;131:1651–8.
72. Buzzi N, Bilbao PS, Boland R, de Boland AR. Extracellular ATP activates MAP kinase cascades through a P2Y purinergic receptor in the human intestinal Caco-2 cell line. Biochimica et biophysica acta [Internet]. Elsevier B.V.; 2009;1790(12):1651–9. Available from: http://www.ncbi.nlm.nih.gov/pubmed/19836435
73. Ghanem E, Robaye B, Leal T, Leipziger J, Van Driessche W, Beauwens R, et al. The role of epithelial P2Y2 and P2Y4 receptors in the regulation of intestinal chloride secretion. British journal of pharmacology [Internet]. 2005;146(3):364–9. Available from: http://www.pubmedcentral.nih.gov/articlerender.fcgi?artid=1576293&tool=pmcentrez&rendertype=abstract
74. Matos JE, Sorensen M V., Geyti CS, Robaye B, Boeynaems JM, Leipziger J. Distal colonic Na+ absorption inhibited by luminal P2Y 2 receptors. Pflugers Archiv European Journal of Physiology. 2007;454(6):977–87.
75. Crane JK, Olson R a, Jones HM, Duffey ME. Release of ATP during host cell killing by enteropathogenic E. coli and its role as a secretory mediator. American journal of physiology Gastrointestinal and liver physiology [Internet]. 2002;283(1):G74–86. Available from: http://www.ncbi.nlm.nih.gov/pubmed/12065294
76. Conway T, Cohen PS. Commensal and Pathogenic Escherichia coli Metabolism in the Gut. Microbiology spectrum [Internet]. NIH Public Access; 2015 Jun [cited 2016 Aug 1];3(3). Available from: http://www.ncbi.nlm.nih.gov/pubmed/26185077

ACKNOWLEDGEMENTS

CLA, GC, VH, VM and PJS are career researchers from Consejo Nacional de Investigaciones Científicas y Técnicas (CONICET). MFLD and NE are CONICET postdoctoral fellowship holders.

MAO is professor at Paris Diderot University.

IMF is PhD student and Monitorat at Universite Paris Diderot Paris 7.

SMM is Researcher from Comisión de Investigaciones Científicas (CIC) of Argentina.The plasmid pGEM3ZF was kindly gifted by Dr. J. Santos (IQUIFIB,

Univ. Buenos Aires). We are grateful to Mario Ramos for designing schemes of Supplementary Figure 2 and Figure 9.
Caco-2 cells were kindly provided by Dra M. Siri, Dr M. Rumbo and Dr E. Cafferata. We are grateful to S. Verstraeten for constructive critics to an early version of the ms, and M.V. Espelt for technical advice regarding cell culture.

FINANCIAL DISCLOSURE

Grant PIP 112 20110100639 and 11220150100459, Consejo Nacional de Investigaciones Científicas y Técnicas. PJS
Grant 20020130100027BA, Universidad de Buenos Aires. PJS
Grant PICT 2014-0327, Agencia Nacional de Promoción Científica y Técnica. PJS
Grant PDTS/CIN 2014 193, Consejo Nacional de Investigaciones Científicas y Técnicas. PJS
ECOS Sud(France)-MINCYT(Argentina) A15S01. PJS-MAO
The funders had no role in study design, data collection and analysis, decision to publish, or preparation of the manuscript.

AUTHOR CONTRIBUTIONS

Conceived and designed the experiments: CLA, GC, NL, IMF, LDMF, NE, SMM, VM, MAO, VH, PJS.
Performed the experiments: CLA, GC, NL, IMF, LDMF, NE, SMM
Analyzed the data: CLA, GC, VM, MAO, VH, PJS.
Contributed reagents/materials/analysis tools: MAO, VM, VH, PJS.
Wrote the paper: CLA, PJS.
Advice on experimental design and hypothesis: VM, VN, MAO
Critical revision of manuscript: MAO, VM, VH

FIGURES AND LEGENDS

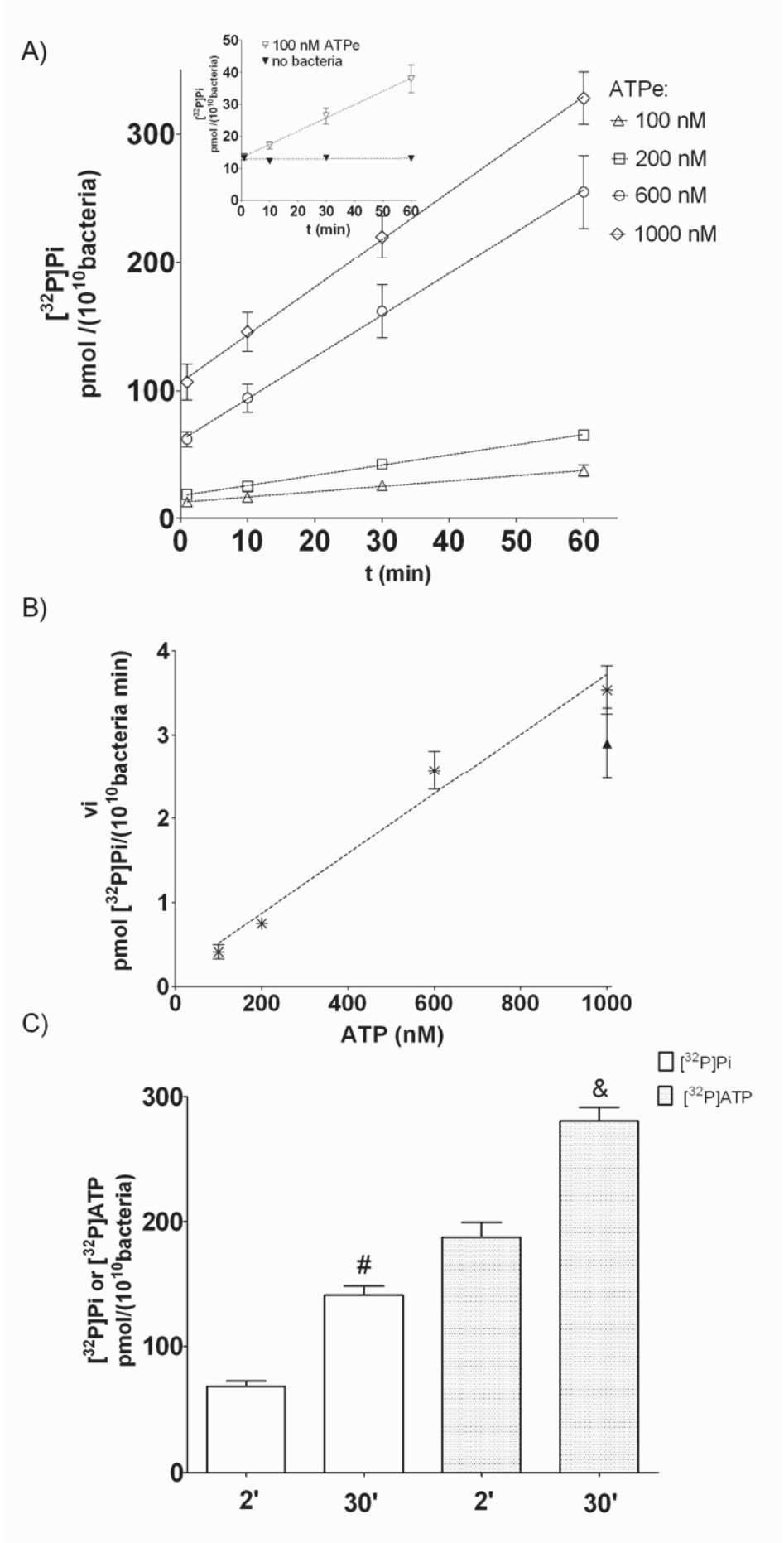
A)
100 nM ATPe
no bacteria
[32P]Pi pmol /(1010bacteria)
t (min)
ATPe:
100 nM
200 nM
600 nM
1000 nM
[32P]Pi pmol /(1010bacteria)
t (min)
B)
vi pmol [32P]Pi/(1010bacteria min)
ATP (nM)
C)
[32P]Pi
[32P]ATP
[32P]Pi or [32P]ATP pmol/(1010bacteria)
#
&
2'
30'
2'
30'

Figure 1: ATPase activity in *E. coli.*

A: Time course of [^{32}P]Pi accumulation released from [γ-^{32}P]ATP (100 -1,000 nM) using *E. coli* suspended in M9 medium.

The dotted lines represent fittings of linear functions to experimental data for each [ATP] used. Results are expressed as pmol [^{32}P]Pi /(10^{10} bacteria), and are means ± SEM (N=6-10, n=12-20).

The inset shows the time course of [^{32}P]Pi accumulation at 100 nM, in media with or without bacteria.

B: ATPase activity (vi) as a function of [ATP]. Each symbol represents ATPase activity calculated as the rate of Pi kinetics using data from A. The dotted line represents the fit of a linear function to experimental data. Results are expressed as pmol [^{32}P]Pi /(10^{10} bacteria min), and are means ± SEM. The triangle symbol represents ATPase activity derived from ATP uptake experiments of C below.

C: Uptake of ATPe. *E. coli* suspensions were exposed to 1 µM [γ-^{32}P]ATP for 2 and 30 min. Results show intracellular concentrations of [γ-^{32}P]ATP or its hydrolysis product [^{32}P]Pi; they are means ± SEM (N=3, n=12) expressed as pmol/(10^{10} bacteria). (& and # denote $p<0.05$ for [γ-^{32}P]ATP and [^{32}P]Pi, respectively).

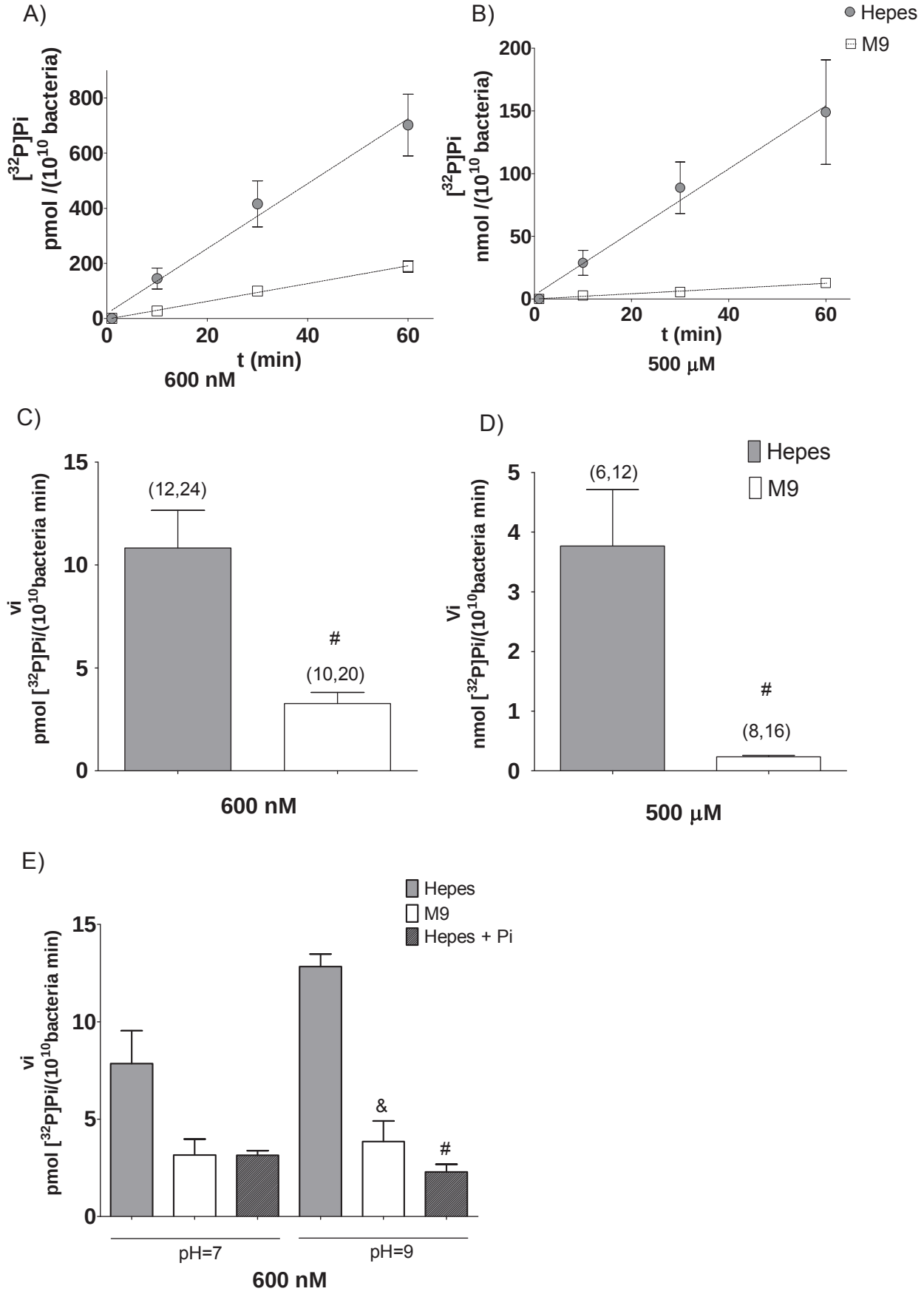
A)
[32P]Pi
pmol /(10^10 bacteria)
800
600
400
200
0
0
20
40
60
t (min)
600 nM
B)
Hepes
M9
[32P]Pi
nmol /(10^10 bacteria)
200
150
100
50
0
0
20
40
60
t (min)
500 µM
C)
vi
pmol [32P]Pi/(10^10bacteria min)
15
10
5
0
(12,24)
#
(10,20)
600 nM
D)
Hepes
M9
Vi
nmol [32P]Pi/(10^10bacteria min)
5
4
3
2
1
0
(6,12)
#
(8,16)
500 µM
E)
Hepes
M9
Hepes + Pi
vi
pmol [32P]Pi/(10^10bacteria min)
15
10
5
0
&
#
pH=7
pH=9
600 nM

Figure 2: Effect of phosphate (Pi) on ATPase activities of *E. coli* suspensions

A: Time course of Pi accumulation ([^{32}P]Pi) released from [γ-^{32}P]ATP (600 nM ATP), using *E. coli* suspended in media with PI (M9, clear symbols) or without Pi (Hepes, gray symbols). The dotted lines represent the fit of linear functions to experimental data. Results are expressed as pmol [^{32}P]Pi /(10^{10} bacteria) (600 nM ATP), and are means ± SEM.

B: Time course of Pi accumulation ([^{32}P]Pi) released from [γ-^{32}P]ATP (500 μM ATP), using *E. coli* suspended in media with phosphate (M9) or without phosphate (Hepes). The dotted lines represent the fit of linear functions to experimental data. Results are expressed as nmol [^{32}P]Pi /(10^{10} bacteria) (500 μM ATP), and are means ± SEM.

C: Rates of Pi accumulation (data from A) were used to calculate ATPase activities (vi). Results are means ± SEM (# $p < 0.001$). Number of replicates (n) and independent experiments (N) are given in brackets on top of the bars (N, n).

D: Rates of Pi accumulation (data from B) were used to calculate apparent maximal activities (Vi). Results are means ± SEM (# $p < 0.001$). Number of replicates (n) and independent experiments (N) are given in brackets on top of the bars (N, n).

E: Effect of Pi and pH on ATPase activity. Rates of Pi accumulation (Supplementary Figure 11) at 600 nM ATP were used to calculate vi. Experiments were run using *E. coli* suspended in media with phosphate (M9, clear symbols), without Pi (Hepes, gray symbols) and Hepes medium containing the same Pi concentration as in M9 medium (Hepes + Pi, gray symbols with hatched lines), both at pH=7 and pH=9. Results are means ± SEM (& $p<0.01$; # $p < 0.001$) of 3 independent experiments with 2 replicates each.

A)

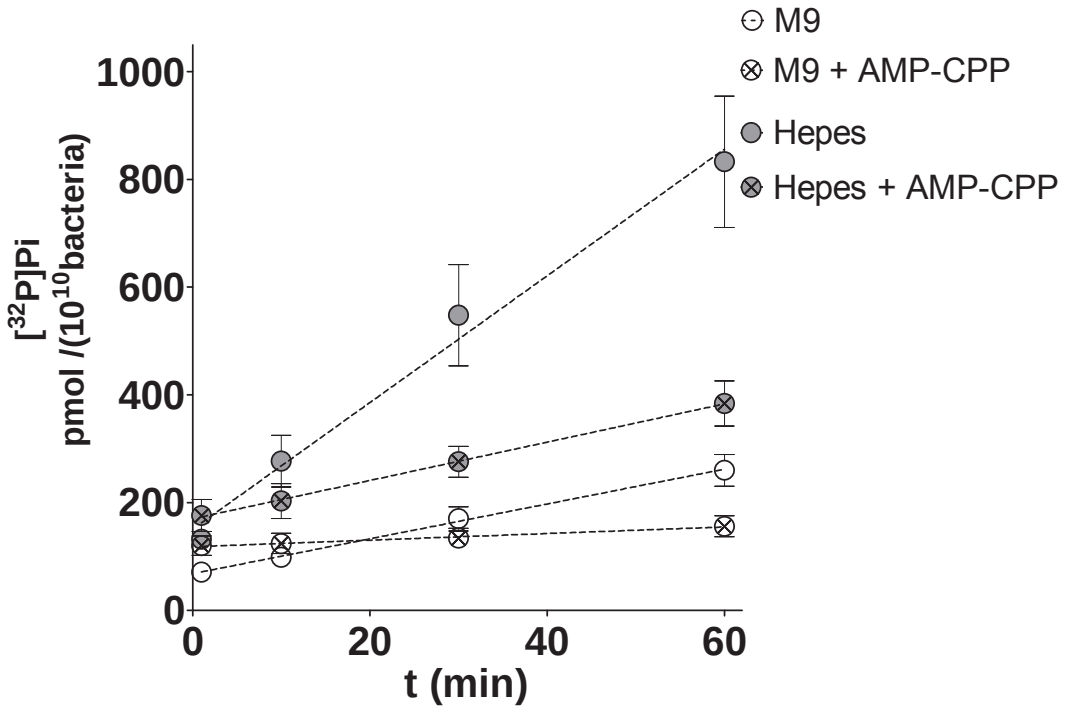
M9
M9 + AMP-CPP
Hepes
Hepes + AMP-CPP
[32P]Pi
pmol /(10^10bacteria)
1000
800
600
400
200
0
0
20
40
60
t (min)

B)

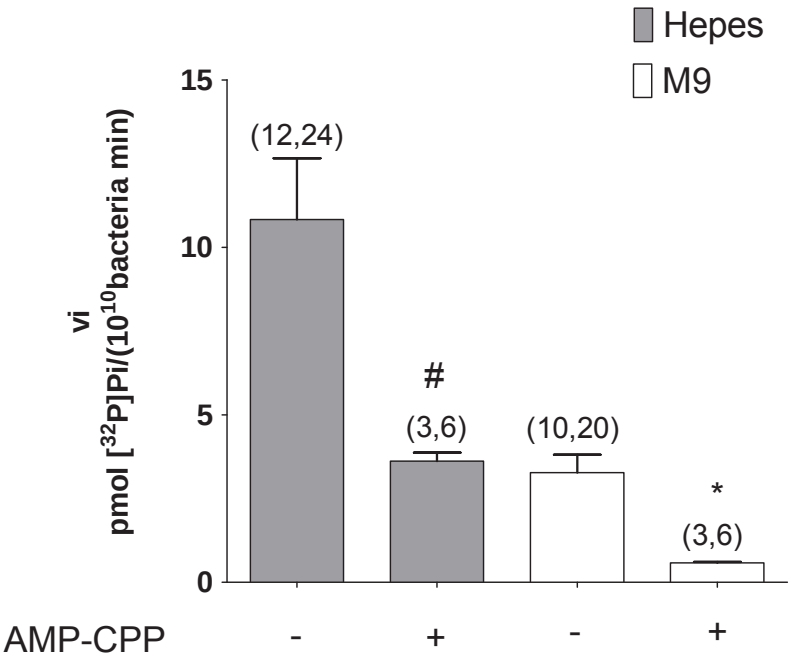
Hepes
M9
vi
pmol [32P]Pi/(10^10bacteria min)
15
10
5
0
(12,24)
#
(3,6)
(10,20)
*
(3,6)
AMP-CPP
-
+
-
+

Figure 3: Effect of AMP-CPP, a non hydrolizable ATP analog, on ATPase activity of *E. coli*.

A: Time course of [^{32}P]Pi accumulation released from 600 nM [γ-^{32}P]ATP, using *E. coli* suspended in media with Pi (M9) or without Pi (Hepes), in the absence or presence of 100 µM AMP-CPP (left). The dotted lines represent the fit of linear functions to experimental data.

B: ATPase activity (vi) derived from Pi kinetics of A. Results are expressed as pmol [^{32}P]Pi /(10^{10} bacteria min) and are means ± SEM. (* $p<0.05$; # $p< 0.001$). Number of replicates (n) and independent experiments (N) are given in brackets on top of the bars (N,n).

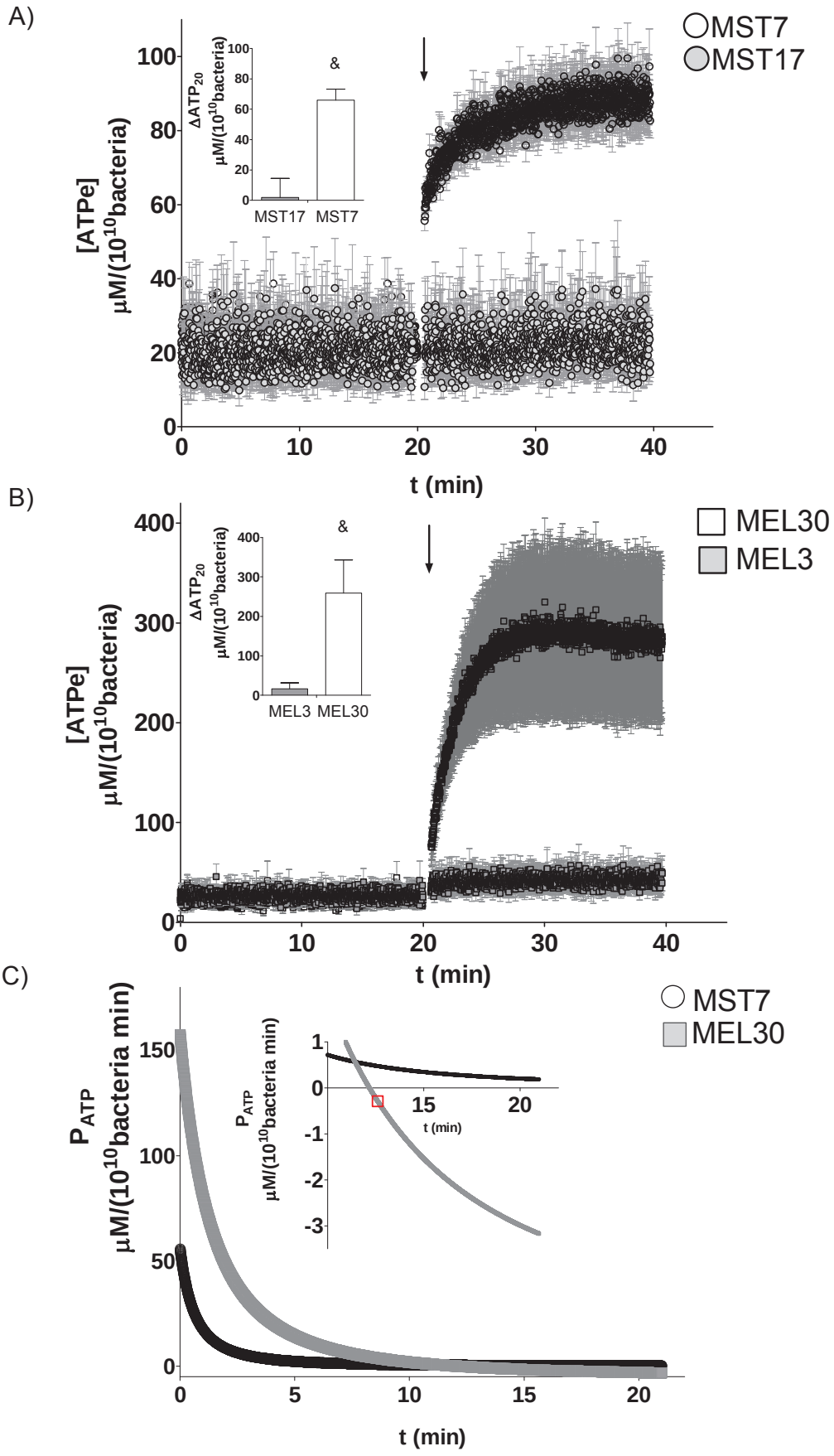
A)
MST7
MST17
[ATPe]
µM/(10^10bacteria)
ΔATP20
µM/(10^10bacteria)
&
MST17 MST7
t (min)
B)
MEL30
MEL3
[ATPe]
µM/(10^10bacteria)
ΔATP20
µM/(10^10bacteria)
&
MEL3 MEL30
t (min)
C)
MST7
MEL30
PATP
µM/(10^10bacteria min)
PATP
µM/(10^10bacteria min)
t (min)
t (min)

Figure 4: ATPe contents, kinetics and permeability of *E. coli* suspensions exposed to mastoparan 7 and melittin.

A-B: Effects of the peptides mastoparan 7 (MST7) and its inactive analog Mastoparan 17 (MST17) (A) or melittin (MEL, B), on ATPe kinetics from *E. coli* suspended in M9 medium.

At the time indicated by the arrow, bacterial suspensions were exposed to:

A. 10 µM of MST7 (N= 12, n=16) and MST17 (N= 5, n=7); B. 3 µM MEL (MEL3, N=5, n=5) or 30 µM MEL (MEL30, N=7, n=7).

Levels of ATPe were expressed as µM/(10^{10} bacteria). Data represent mean values ± SEM.

Insets of Figures A-B: Data of A and B were used to calculate the increase of [ATPe] at 20 min post-stimulus. Values are expressed as ΔATP_{20} [µM/(10^{10} bacteria)], i.e., the difference between [ATPe] at 20 min post-stimulus and basal [ATPe]. Results are means ± SEM. (& $p<0.01$).

C: Data of A and B were used to calculate the effects of MST7 and MEL30 on ATP permeability (P_{ATP}). Values are expressed as µM/(10^{10} bacteria min). Inset: a detail of the last 5 min of the experiments. For the MEL30 curve, the red dot indicates the time point when ATPe decays equals ATPase activity (vi) derived from Figure 1B at 290 nM.

A)

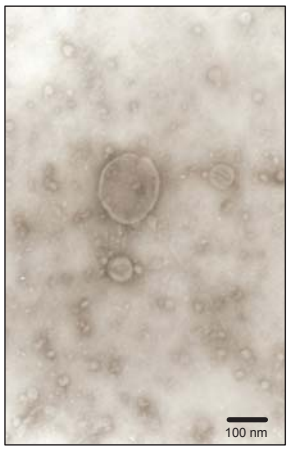
100 nm

C)

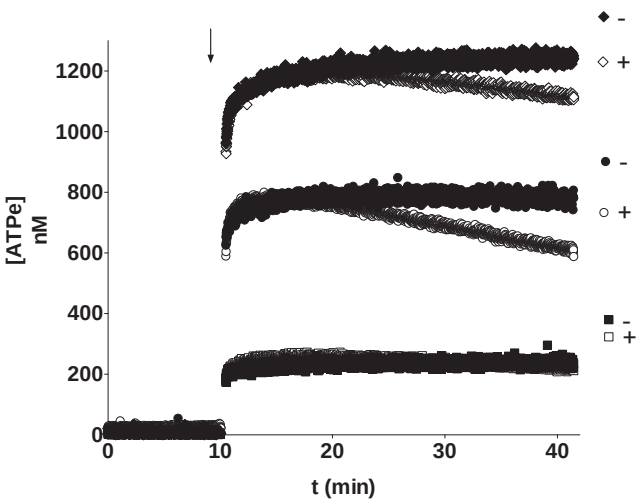
[ATPe] nM
1200
1000
800
600
400
200
0
0
10
20
30
40
t (min)
-
+
-
+
-
+

B)

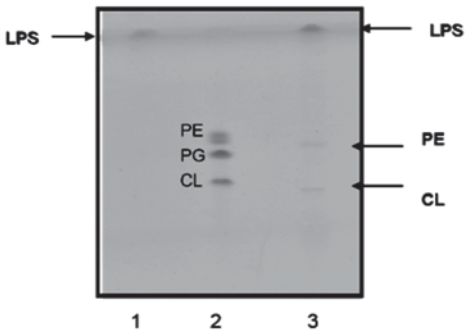
LPS
LPS
PE
PG
CL
PE
CL
1
2
3

D)

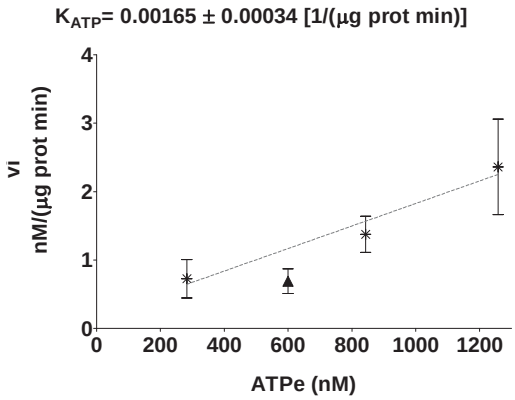
K_ATP= 0.00165 ± 0.00034 [1/(µg prot min)]
vi nM/(µg prot min)
4
3
2
1
0
0
200
400
600
800
1000
1200
ATPe (nM)

Figure 5: Outer Membrane Vesicles (OMVs) from *E. coli*. Morphology, lipid composition, ATPe kinetics and ATPase activity.

A: Electron micrographs (50,000 X) of OMVs. Scale bars are 100 nm.

B: Thin Layer Chromatography of OMVs. 1: LPS extracted from *E. coli*; 2: standard lipids: Phosphatidylglicerol (PG), cardiolipin (CL) and phosphatidylethenolamine (PE) and 3: total lipids extracted from OMVs.

C: ATPase kinetics of OMVs exposed to exogenous ATP. Experiments were run in the presence of OMVs (white symbols) or –controls- in their absence (solid symbols). At the time indicated by the arrow, ATP was added at 200 nM (□, N=4, n=4), 600 nM (○, N=6, n=6) and 1,000 nM (◊, N=5, n=5). Levels of ATPe were expressed as nM for µg OMVs suspended in 100 µl assay medium (0.8-1.4 µg protein per experiment). +: with OMVs; -: without OMVs. Mean values are shown.

D: ATPase activity as nM /(µg prot min) of OMVs. Each symbol was calculated from the initial rate of [ATPe] decay taken from data of C. ATPe values of the abscisa result from the sum of endogenous + exogenous ATP. The dotted line is a fit of a linear function to experimental data. The solid triangle represents a result from an independent experiment (data of Supplementary Figure 6) where ATPase activity was determined by following the time course of [^{32}P]Pi released from [γ-^{32}P]ATP 600 nM. Results are means ± SEM.

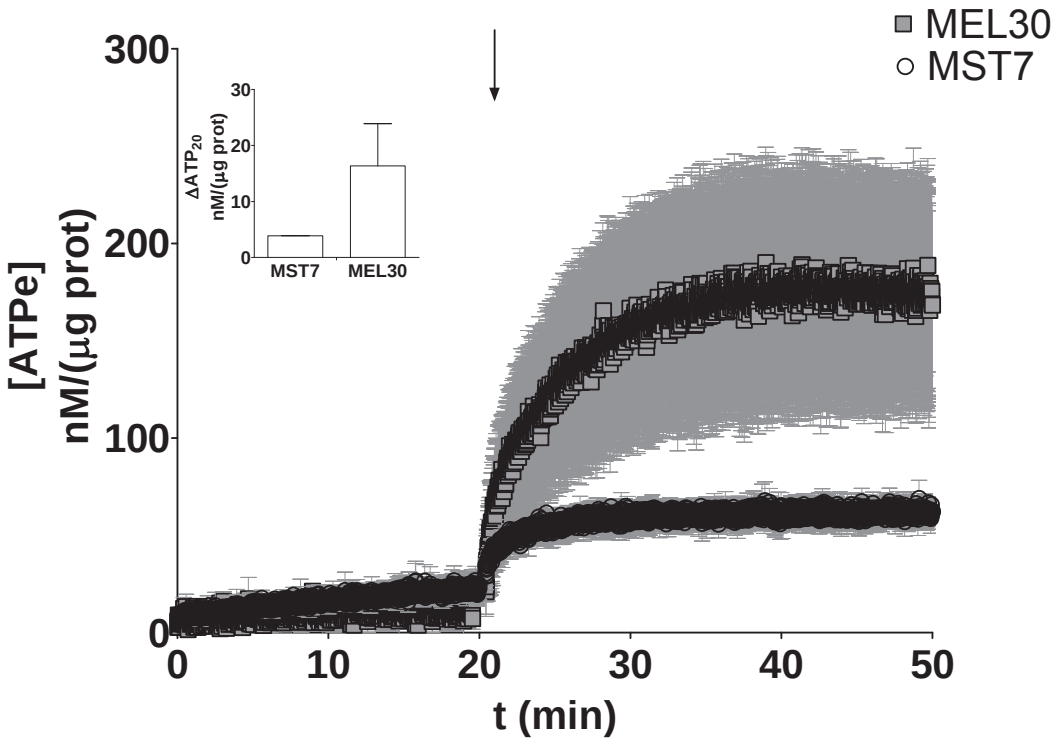
MEL30
MST7
[ATPe]
nM/(µg prot)
300
200
100
0
0
10
20
30
40
50
t (min)
ΔATP20
nM/(µg prot)
30
20
10
0
MST7
MEL30

Figure 6: ATPe kinetics of Mastoparan 7- and Melittin-treated OMVs.
The time course of [ATPe] was quantified by real time luminometry, similarly to Figure 4. At the time indicated by the arrow, OMVs were exposed to 10 µM MST7 or 30 µM melittin (MEL30). Levels of ATPe were expressed as nM/(µg prot). Data represent mean values ± SEM (N=2, n=6). Experiments in which OMVs were exposed to 30 µM melittin for more prolonged times are shown in Supplementary Figure 7.
Inset: Data were used to calculate the increase of [ATPe] at 20 min post-stimulus. Values are expressed as ΔATP_{20} [nM/(µg prot)], i.e., the difference between [ATPe] at 20 min post-stimulus and basal [ATPe].

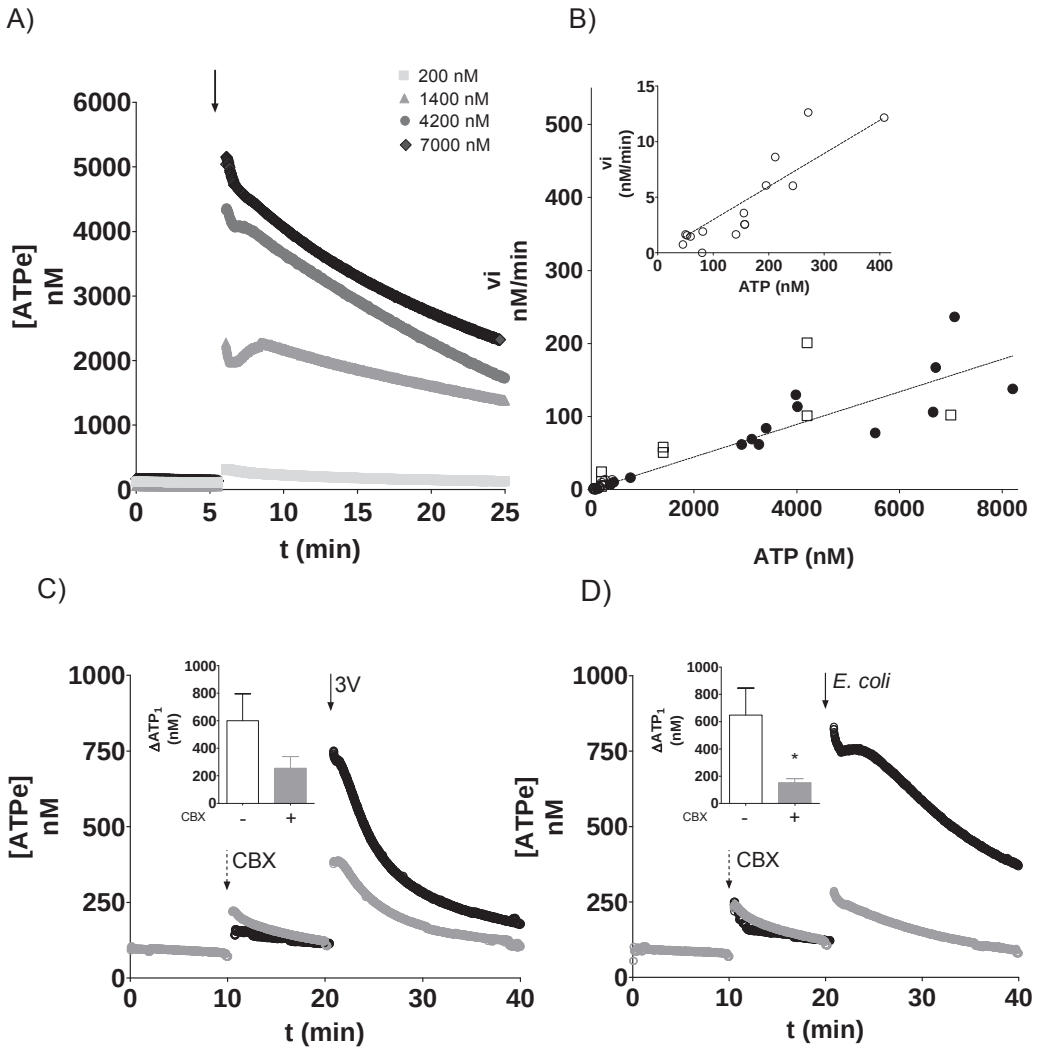
A)
B)
C)
D)
200 nM
1400 nM
4200 nM
7000 nM
[ATPe] nM
t (min)
vi nM/min
ATP (nM)
vi (nM/min)
3V
CBX
ΔATP1 (nM)
E. coli

Figure 7: ATPe kinetics and ectoATPase activity of Caco-2 cells.
Assessment of ATPe kinetics by luminometry (section 10.3) and ectoATPase activity by [γ-^{32}P]Pi production(section 10.1) on the apical side of polarized Caco-2 cells.
A. ATPe kinetics of cells exposed to exogenous ATP (200-7000 nM). Levels of ATPe are mean values expressed as nM for approximately 5x10^5 cells incubated in 40 µl of apical medium (N=3-6).
B. ATPase activities (vi) were estimated from ATPe decay kinetics using data from A (circles), or from [^{32}P]Pi production from [γ-^{32}P]ATP (squares), using data from Supplementary Figure 9. Results are expressed as nM/min. Open and closed circles represent vi values calculated from ATPe kinetics in the absence and presence of exogenous ATP, respectively. The dotted line represents the fitting of a linear function to experimental data. The inset shows a detail of the low range of ATPe concentrations (0-400 nM).

C. ATPe kinetics of cells exposed to the adrenergic cocktail 3V (30 µM forskolin, 100 µM papaverine, 10 µM isoproterenol). Experiments were run in the absence (black lines) and presence (grey lines) of 100 µM carbenoxolone (CBX). Levels of ATPe are mean values expressed as nM (N=11).
D. ATPe kinetics of cells exposed to *E. coli* suspensions. Experiments were run in the absence (black lines) and presence (grey lines) of 100 µM CBX. Levels of ATPe are mean values expressed as nM (N=10-12).
Insets of Figures C and D. Apical ATPe levels taken from data of C and D. Values are expressed as ΔATP_1, i.e., the difference between [ATPe] at 1 min post-stimulus and basal [ATPe]. Results are means ± SEM (* $p<0.05$).
Each filter containing polarized monolayers of Caco-2 cells was considered an independent preparation (N)

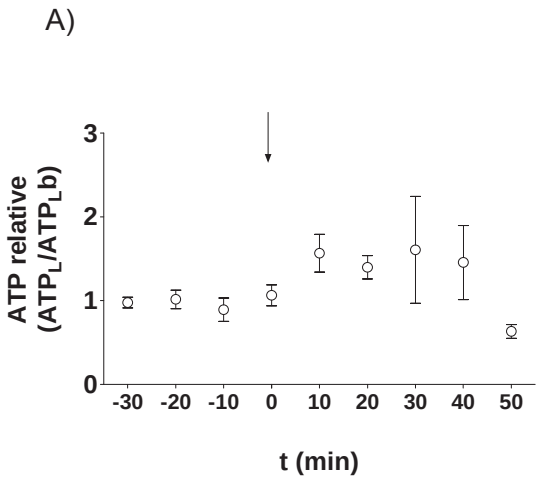
A)
ATP relative
(ATP$_L$/ATP$_L$b)
3
2
1
0
-30 -20 -10 0 10 20 30 40 50
t (min)

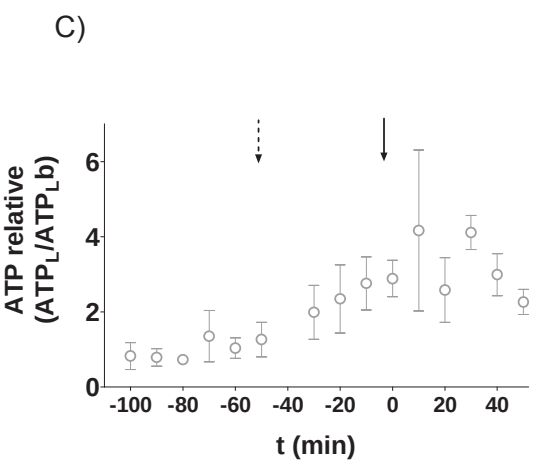
C)
ATP relative
(ATP$_L$/ATP$_L$b)
6
4
2
0
-100 -80 -60 -40 -20 0 20 40
t (min)

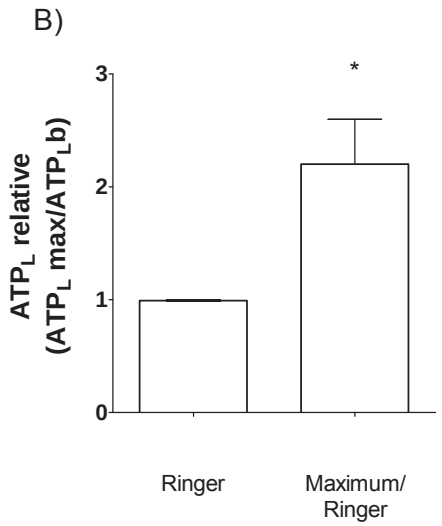
B)
ATP$_L$ relative
(ATP$_L$ max/ATP$_L$b)
3
2
1
0
*
Ringer
Maximum/
Ringer

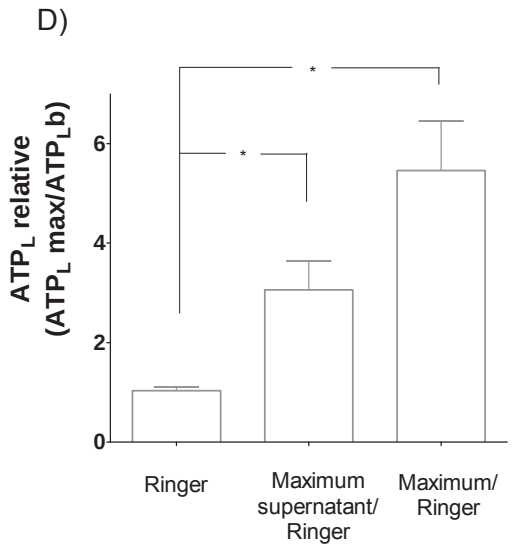
D)
ATP$_L$ relative
(ATP$_L$ max/ATP$_L$b)
6
4
2
0
*
*
Ringer
Maximum
supernatant/
Ringer
Maximum/
Ringer

Figure 8. Luminal ATP contents of rat intestinal segments

A. The time course of luminal ATP (ATP_L) from rat jejunum segments was followed by off-line luminometry (section 8.2). At the time indicated by the arrow, bacterial suspensions (final concentration $5x10^8$ bacteria / mL) were perfused in rat intestinal segments. Data represent mean values ± SEM (N=4).

B: Maximal ATP_L concentrations (maximum) attained during bacterial perfusion. Values were normalized with respect to control ATP_L values (basal) in the absence of bacteria ($p<0.05$, N=4).

C. The time course of luminal ATP (ATP_L) from rat jejunum segments was followed by off-line luminometry (section 8.2). At the time indicated by the dashed line arrow, supernatants collected from *E. coli* suspensions were perfused in intestinal segments. The continuous arrow represents the time at which bacterial suspensions were perfused (final concentration $5x10^8$ bacteria/mL). Data represent mean values ± SEM (N=3).

D: Maximal ATP_L concentrations attained during supernatant (maximum supernatant) and bacterial (maximum) perfusion. Values were normalized with respect to control ATP_L values (Ringer) (* $p<0.05$).

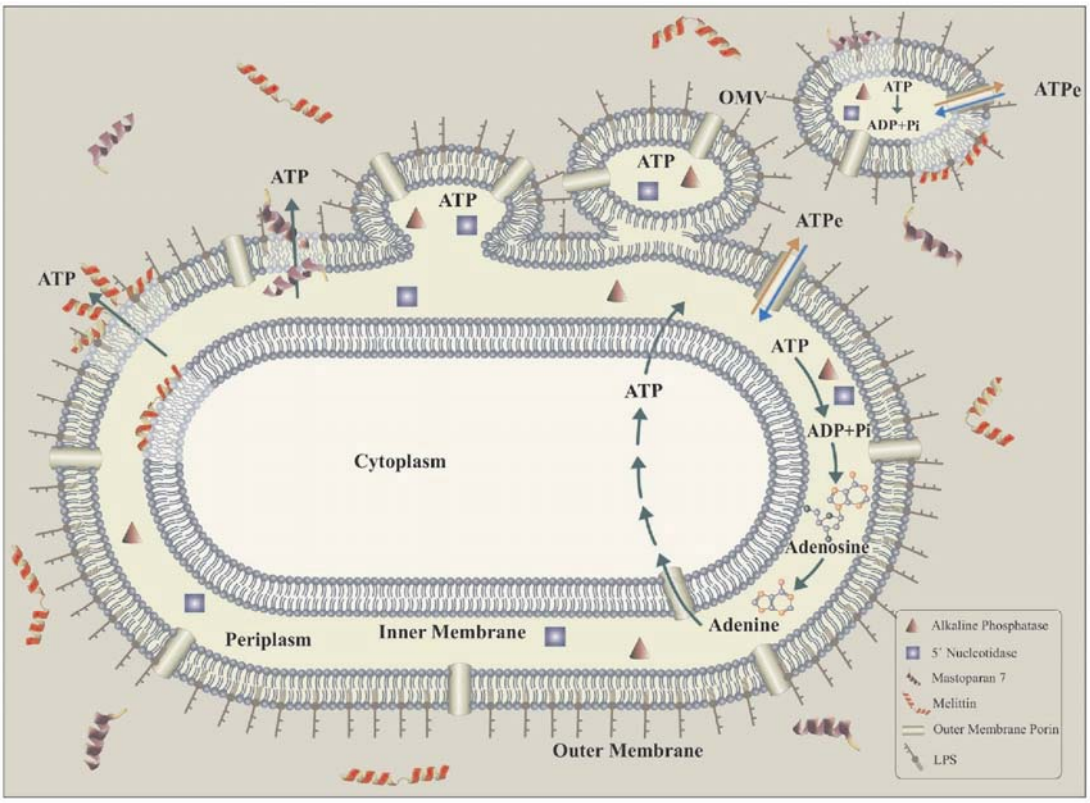
OMV
ATP
ADP+Pi
ATPe
ATP
ATP
ATP
ATPe
ATP
ATP
ATP
ADP+Pi
Cytoplasm
Adenosine
Adenine
Periplasm
Inner Membrane
Outer Membrane
Alkaline Phosphatase
5' Nucleotidase
Mastoparan 7
Melittin
Outer Membrane Porin
LPS

Figure 9: Qualitative model of ATPe regulation of *E. coli* and their Outer Membrane Vesicles (OMVs).

Under normal growth conditions, OMVs are continuously formed from *E. coli*. These spherical vesicles form when small portions of the outer membrane bulge away from bacteria grown in broth, pinch off and release.

ATP can be present in the cytosol, the periplasm, the extracellular space or the lumen of OMVs. Permeabilizers can act on the OM alone (MST7) or both on the outer and inner membrane (MEL).

E. coli was shown to hydrolyze ATPe and, in the presence of amphipatic peptides, release ATP. Since during formation OMVs encapsulate portions of the bacterial periplasm with soluble proteins, they might exhibit ATPase activity due to –originally periplasmic- nucleotidases and phosphatases.

In both, OMVs or bacteria, regulation of ATPe depends on the dynamic balance between the rates of ATP hydrolysis, facilitated by nucleotidases/phosphatases of the periplasm (*E. coli*) or vesicular lumen (OMVs) and of ATP release induced by MST7 and MEL.